Title:

Molecular mechanisms of selenium tolerance and hyperaccumulation in *Stanleya pinnata*

Authors:

John L. Freeman[1,2,3]*, Masanori Tamaoki[4]*, Cecil Stushnoff[5], Colin F. Quinn[1], Jennifer J. Cappa[1], Jean Devonshire[6], Sirine C. Fakra[7], Matthew A. Marcus[7], Steve P. McGrath[6], Doug Van Hoewyk[1,8] and Elizabeth A.H. Pilon-Smits[1]

[1] Colorado State University, Biology Department, Fort Collins, CO 80523, USA

[2]United States Department of Agriculture, Agricultural Research Service, Water Management Research Division, Parlier CA 93648, USA

[3]California State University Fresno, Center for Irrigation Technology, Fresno CA, 93740, USA

[4]National Institute for Environmental Studies, Environmental Biology Division, Tsukuba, Ibaraki 305-8506, Japan

[5]Colorado State University, Department of Horticulture and Landscape Architecture, Fort Collins, CO 80523, USA

[6]Rothamsted Research, Harpenden, Herts, AL5 2JQ, UK

[7]Advanced Light Source, Lawrence Berkeley Laboratory, Berkeley, CA 94720, U.S.A.

[8]Coastal Carolina University, Department of Biology, PO Box 261954, Conway, SC 29526

*Authors contributed equally to this paper

Footnotes:

This work was supported by grants from the National Science Foundation (grants no. IOB-0444471 and IOS-0817748 to E.P.S.) and the Ministry of Education, Science, Sports and Culture of Japan (grant no. 18780006 to M.T.). Corresponding author; Elizabeth A.H. Pilon-Smits, e-mail epsmits@lamar.colostate.edu

Abstract

The molecular mechanisms responsible for selenium (Se) tolerance and hyperaccumulation were studied in the Se hyperaccumulator *Stanleya pinnata* (Brassicaceae) by comparing it to the related secondary Se accumulator *S. albescens* using a combination of physiological, structural, genomic and biochemical approaches. *S. pinnata* accumulated 3.6-fold more Se and was tolerant to 20 µM selenate while *S. albescens* suffered reduced growth, chlorosis and necrosis, impaired photosynthesis and high levels of reactive oxygen species. Levels of ascorbic acid, glutathione, total sulfur and non-protein thiols were higher in *S. pinnata*, suggesting that Se-tolerance may in part be due to increased antioxidants and upregulated sulfur assimilation. *S. pinnata* had higher selenocysteine methyltransferase protein levels and, judged from LCMS, mainly accumulated the free amino acid methylselenocysteine while *S. albescens* accumulated mainly the free amino acid selenocystathionine. *S. albescens* leaf XANES scans mainly detected a C-Se-C compound (presumably selenocystathionine), in addition to some selenocysteine and selenate. Thus *S. albescens* may accumulate more toxic forms of Se in its leaves than *S. pinnata*. The species also showed different leaf Se sequestration patterns: while *S. albescens* showed a diffuse pattern, *S. pinnata* sequestered Se in localized epidermal cell clusters along leaf margins and tips, concentrated inside of epidermal cells. Transcript analyses of *S. pinnata* showed a constitutively higher expression of genes involved in sulfur assimilation, antioxidant activities, defense, and response to (methyl)-jasmonic acid, salicylic acid or ethylene. The levels of some of these hormones were constitutively elevated in *S. pinnata* compared to *S. albescens*, and leaf Se accumulation was slightly enhanced in both species when these hormones were supplied. Thus, defense-related phytohormones may play an important signaling role in the Se hyperaccumulation of *S. pinnata* perhaps by constitutively up-regulating sulfur/selenium assimilation followed by methylation of selenocysteine and the targeted sequestration of methylselenocysteine.

Introduction

Selenium (Se) is an essential micronutrient for many organisms, but for higher plants an essential function of Se has not yet been discovered (Zhang and Gladyshev, 2009). Most plant species accumulate less than 25 μg Se g^{-1} dry weight (DW) in their natural environment and cannot tolerate increased Se concentrations; these are termed non-accumulators (White et al., 2004). In contrast, some species of the genera *Stanleya* (Brassicaceae) and *Astragalus* (Fabaceae) can hyperaccumulate Se to concentrations of 1,000–15,000 μg Se g^{-1} DW in their shoots (0.1-1.5%) while growing on soils containing only 2–10 μg Se g^{-1} DW (Byers, 1935; Virupaksha and Shrift, 1965; Davis, 1972, 1986; Galeas et al., 2007). Hyperaccumulation is a phenomenon where plants accumulate metals or metalloids to much higher concentrations compared to non-accumulator plants, typically >100 fold when growing in their natural habitat on metalliferous soils (Minguzzi and Vergnano, 1948; Jaffre et al., 1976; Brooks et al., 1977). Metals that can be hyperaccumulated by plants include Ni, Zn, Co, Cr, Mo, Cd, As, and Se (Reeves and Baker, 2000). To date 45 plant families are documented to contain hyperaccumulators, and at least 200 metal hyperaccumulating species have evolved worldwide (Reeves and Baker, 2000). Hyperaccumulators typically have shoot-to-root metal ratios >2, and their leaves often show the highest metal concentration inside specific tissues such as epidermal cells or leaf hairs and most often inside large or small vacuoles (Krämer et al., 1997; Küpper et al., 1999, 2000 and 2001, Pickering et al., 2003a, Freeman et al., 2006, reviewed by Peer et al., 2005). Both metal tolerance and hyperaccumulation are considered prerequisites for metal hyperaccumulation in plants and these molecular mechanisms have been found to be under independent genetic control (Macnair et al., 1999; Assucao et al., 2003; Bert et al., 2003).

Environmental factors influencing the evolution of elemental hyperaccumulation in plants have been hypothesized to be metal tolerance, allelopathy, drought tolerance or protection from herbivores and pathogens (Tadros, 1957; Reeves and Brooks, 1983; Baker and Brooks, 1989; Boyd and Martens, 1992; Baker and Whiting, 2002; Boyd, 2007). Depending on the plant species and the metal, different selection pressures may have resulted in the hyperaccumulator phenotype. Most studies investigating the effect of Se hyperaccumulation on herbivores and pathogens have supported a function for Se in defense (Boyd, 2007; Pilon-Smits and Freeman,

2006; Quinn et al., 2007). This phenomenon is termed the elemental defense hypothesis and has been shown in a wide range of hyperaccumulator species for many different metals (Boyd and Martens, 1992; Boyd, 2007). The hyperaccumulators *Astragalus bisulcatus* and *Stanleya pinnata* were found to predominantly accumulate Se in peripheral tissues of young leaves and reproductive organs: in structures important to protect, prone to herbivore and pathogen attacks, and/or typically associated with playing a defensive role (Pickering et al., 2004, Freeman et al., 2006a; Galeas et al., 2007). Indeed, laboratory and field studies have shown that Se can protect plants from various herbivores and fungal pathogens (Vickerman and Trumble, 1999; Hanson et al., 2003, 2004; Banuelos et al., 2002; Freeman et al., 2006b, 2007, 2009; Galeas et al., 2008; Quinn et al., 2008).

Selenium is chemically similar to sulfur (S) and is assimilated by S metabolic pathways. Plants take up selenate (SeO_4^{2-}), the most abundant bioavailable form of Se in soils via sulfate transporters in roots (Shibagaki et al., 2002). After uptake selenate is thought to be transported into leaves and chloroplasts (Leustek, 2002). Indistinguishable to most S enzymes, Se can be found in most S- containing metabolites (Leustek 2002). In chloroplasts the S assimilation pathway first reduces selenate to selenite, then selenide, which is enzymaticaly incorporated into selenocysteine (SeCys) and selenomethionine (SeMet) (for reviews see Terry et al., 2000; Sors et al., 2005). These two seleno-amino acids can be misincorporated into proteins, replacing Cys and Met, which causes Se toxicity (Brown and Shrift, 1981, 1982; Stadtman, 1996). It has also been shown that Se causes ROS formation and oxidative stress in plants (Gomes-Junior, 2007; Tamaoki et al., 2008a). Selenium toxicity in plants may directly result from the ROS generated via selenite reacting with reduced glutathione, as shown *in vitro* (Saitoh and Imuran, 1987). Alternatively, Se toxicity could result if Se replaces S in essential S-metabolites including proteins.

A key enzyme in Se hyperaccumulators is selenocysteine methyltransferase (SMT), which methylates SeCys and prevents it from being misincorporated into proteins, thereby preventing toxicity (Brown and Shrift, 1981, 1982; Neuhierl and Bock, 1996). Thus, the hyperaccumulator *A. bisulcatus* rapidly converts selenate to methylselenocysteine (MeSeCys) (Virupaksha and Shrift, 1965; Dunnhill and Fowden, 1967) and γ-glutamyl-methylselenocysteine (γGMeSeCys) (Nigam and McConnell, 1969; Freeman et al., 2006a). The gene encoding SMT was cloned from *A. bisulcatus* (Neuhierl and Bock 1996) and overexpressed in *Arabidopsis thaliana* (*A. thaliana*) and *Brassica juncea*; this led to enhanced Se tolerance and accumulation when plants were given selenite (SeO_3^{2-}), but not when given selenate (Ellis et al., 2004; LeDuc et al., 2004). Total Se accumulation in the SMT transgenic plants was much lower than

commonly found in hyperaccumulators, which suggests that SMT is an important enzyme for hyperaccumulation and tolerance, but additional processes are involved that have a synergistic effect on Se hyperaccumulation. Sors et al. (2005) found no evidence that enzymatic differences in the capacity to reduce or assimilate S is important for Se hyperaccumulation in *Astragalus*, while SMT enzyme activity correlated with Se hyperaccumulation. Additionally, a non-accumulator SMT homologue lacked the SMT activity *in vitro*, explaining why little or no detectable MeSeCys accumulation was observed in the non-accumulator species (Sors et al., 2009). The SMT enzyme is now known to be localized predominantly within the chloroplast in *Astragalus*, the principal site of Se and S assimilation in plants (Sors et al., 2009). Like *A. bisulcatus*, the Brassicaceae hyperaccumulator *S. pinnata* accumulates mainly MeSeCys (Shrift and Virupaksha 1965; Freeman et al., 2006a). In addition to the specific methylation of SeCys by SMT it is not clear at this point which mechanisms may contribute to Se hyperaccumulation and tolerance in *A. bisulcatus* or other hyperaccumulators (Sors et al., 2005, 2009). Selenium hyperaccumulators do possess some unexplained physiological traits associated with growing on Se-enriched soils. *Stanleya pinnata* roots have been reported to grow toward Se-rich soil in split box experiments, and *Astragalus* species have been documented to grow slower and are smaller in the absence of Se in soils (Goodson et al., 2003, Trelease and Beath 1949, Trelease and Trelease 1938).

There is substantial variation in Se accumulation (ranging from hyperaccumulation to Se secondary accumulation to Se non-accumulation) and Se tolerance between and within *Stanleya* species (Beath et al., 1939; Feist and Parker, 2001) making it an ideal genus to compare molecular mechanisms involved in Se hyperaccumulation and tolerance. In the current study we compare Se tolerance and hyperaccumulation between the hyperaccumulator *S. pinnata* (Pursh) Britton var. pinnata (prince's plume) and the secondary accumulator *Stanleya albescens* (M.E. Jones) (white prince's plume). We investigated the molecular mechanisms responsible for Se tolerance and hyperaccumulation using a combination of molecular, structural, genomic, biochemical and physiological analyses. Together, our new findings give better insight into the underlying molecular mechanisms associated with Se hyperaccumulation in *S. pinnata*.

Results

Se tolerance assay

Selenium tolerance in *S. pinnata* and *S. albescens* was first tested in seedlings by measuring root growth on vertically placed agar plates after 30 d of growth from germination (Supplemental

Figure 1). The relative tolerance index (RTI) was calculated by dividing root length of seedlings grown with 40 μM selenate by the average root length of the same species grown without Se. The RTI was 2.6 for the Se hyperaccumulator *S. pinnata* and 0.6 for *S. albescens*. Thus, *S. pinnata* appeared to benefit from 40 μM selenate in its growth medium ($P < 0.01$), while *S. albescens* was impaired by it ($P = 0.063$). When grown with 40 μM selenate, *S. pinnata* roots were 1.6 times longer than *S. albescens* roots ($P < 0.05$). When grown without Se the roots of *S. pinnata* were 2.6 fold shorter than those of *S. albescens* ($P < 0.05$).

Selenium tolerance of the two species was then compared in more mature plants. After 16 weeks of semi-arid drip system growth in the presence of 20 μM selenate *S. pinnata* showed no signs of Se toxicity (Figure 1A) but had the same phenotype as *S. pinnata* grown without Se (Figure 1B). However, *S. albescens* grown with Se showed visible leaf chlorosis and necrosis (Figure 1C). This phenotype was not present in *S. albesens* grown without selenate (Figure 1D). Thus, both at the seedling and mature plant level, *S. pinnata* was completely tolerant to, or even benefited from 20 μM selenate, while *S. albescens* was sensitive to this Se treatment.

Selenium and sulfur accumulation

After 10 weeks of growth from germination in the presence of 20 μM selenate, *S. pinnata* had 2.6-fold higher levels of Se in its leaves than *S. albescens*, and after 16 weeks *S. pinnata* leaf Se levels were 3.6-fold higher than those in *S. albescens* (2,973 ± 446 μg Se g^{-1} DW and 818 ± 49 μg Se g^{-1} DW respectively, Figure 1E). After 16 weeks of growth with Se, the roots of *S. pinnata* contained 721 μg Se g^{-1} DW, a 3.6-fold higher Se concentration compared to the roots of *S. albescens*, which contained 201 μg Se g^{-1} DW.

These Se levels in *S. pinnata* confirm that this species is a Se hyperaccumulator, and are comparable to those found in its native habitat on seleniferous soil West of Fort Collins, Colorado, where *S. pinnata* leaves from ten individuals averaged 3,775 ± 506 μg Se g^{-1} DW (Galeas et al., 2007). *Stanleya albescens* does not appear to be a hyperaccumulator, based on these results and from field collection data (DNS) but rather resembles a typical secondary accumulator of Se, such as *Brassica juncea*.

Since selenate and sulfate compete for uptake and assimilation in plants, the S levels in *S. pinnata a*nd *S. albescens* were also compared. After 16 weeks of growth with Se, *S. pinnata* had accumulated 1.3-fold more S than *S. albescens*: 7,235 ± 279 μg S g^{-1} DW compared to 5,391 ± 32 μg S g^{-1} DW ($P < 0.05$). Grown without Se the two species showed little or no significant difference in leaf sulfur concentration: *S. pinnata* accumulated 13,728 ± 888 μg S g^{-1} DW while

S. albescens accumulated 11,169 ± 431 μg S g^{-1} DW. Both species accumulated twice as much S when grown without Se compared to selenate-supplied plants of the same species. The direct comparison of μg Se g^{-1}DW/ μg S g^{-1} DW in leaves of Se-supplied plants showed a ratio of 0.43 for *S. pinnata* and 0.19 for *S. albescens*. Thus, despite its higher S levels the hyperaccumulator still had a higher Se/S ratio. For comparison, the selenate/sulfate ratio in the supplied medium was around 0.05.

Reduced organic S metabolites have been reported to compose a large fraction of the S pool (Nikiforova et al., 2006). To determine whether levels of reduced organic S metabolites differed between the species and how they are affected by selenate treatment, the levels of total non-protein thiols (reduced S metabolites including glutathione and cysteine) were measured in young and mature leaves of *S. pinnata* and *S. albescens* grown with and without Se (supplemental Figure 2). Mature leaves of *S. pinnata* plants supplied with Se contained 60% higher non-protein thiol levels compared to the mature leaves of *S. albescens* ($P < 0.05$); there were no significant differences between the two species when the plants were grown without Se.

Effects of Se on leaf physiology

As a further comparison of Se tolerance in the two species, the effect of 20 μM selenate on the photosynthetic efficiency of *S. pinnata* and *S. albescens* was analyzed after 16 weeks of growth. The light-dependent electron transport rate was highest for *S. pinnata* treated with Se, followed by *S. pinnata* and *S. albescens* grown without Se (Figure 2). The lowest photosynthetic rate was observed for *S. albescens* grown with Se.

Reactive oxygen species (ROS) are formed when stress or malfunctions impede electron flow in the photosynthetic electron transport chain. A Se-associated reduction in electron flux like that observed for *S. albescens* may therefore give rise to ROS production. Increased ROS may also be formed directly from selenite and reduced glutathione *in vitro* (Saitoh and Imuran, 1987). Selenium treatment has been shown previously to induce ROS accumulation in *A. thaliana* leaves and coffee cells (Gomes-Junior, 2007; Tamaoki et al., 2008a). The production of ROS in the two *Stanleya* species was analyzed *in situ* using stains sensitive to superoxide and hydrogen peroxide. In plants treated with 20 μM selenate for ten weeks the superoxide accumulation in *S. pinnata* leaves was lower compared to *S. albescens* leaves (Figure 3A, B). Similarly, the hydrogen peroxide accumulation in leaves of *S. pinnata* treated with 20 μM selenate for ten weeks was lower compared to *S. albescens* leaves grown with Se (Figure 3C, D). Thus, when grown with Se *S. pinnata* photosynthesis was not negatively affected and ROS were

not accumulated. However, *S. albescens* photosynthesis was negatively affected when grown with Se and superoxide and hydrogen peroxide radicals accumulated. These results confirm that the secondary accumulator *S. albescens* is sensitive to 20 μM selenate while the hyperaccumulator *S. pinnata* is not.

Quantification of antioxidant and ROS scavenging capacity

The observed differences between *S. pinnata* and *S. albescens* in Se-induced ROS led us to investigate the levels of the important antioxidant glutathione in young leaves from both species (Figure 4A). When grown without Se *S. pinnata* contained 1.2-fold more reduced glutathione (GSH), 4.3-fold more oxidized glutathione (GSSG) and 1.4-fold more total glutathione (GSH+GSSG) than *S. albescens* ($P < 0.05$). When grown with Se *S. pinnata* contained a 1.4-fold higher level of GSH, a 1.2-fold higher GSSG level and a 1.3-fold higher total glutathione level than *S. albescens* ($P < 0.05$). The glutathione redox state (ratio of reduced to oxidized glutathione) in plants grown without Se was 3.6 for *S. pinnata* and 13.2 (a relatively normal ratio) for *S. albescens*, while plants grown with Se showed a ratio of 4.0 for *S. pinnata* and 3.4 for *S. albescens* (Figure 4A). Thus, in the Se-sensitive species *S. albescens* there was a significant drop in the reduction state of its glutathione pool when treated with 20 μM selenate ($P < 0.05$), while in the Se-tolerant *S. pinnata* the ratio of reduced to oxidized glutathione was unaffected. In both species treatment with Se caused a significant concentration decrease in total glutathione relative to plants grown without Se ($P < 0.05$).

In order to further examine antioxidant levels we measured ascorbic acid (AsA) concentrations in young leaves of both species, another important antioxidant molecule in plants (Smirnoff et al., 2001). When grown without Se, *S. pinnata* had a 1.3-fold higher AsA concentration than *S. albescens* ($P < 0.05$, Figure 4B), but when grown with Se no significant difference in AsA concentration was observed between the species. Taken together, these findings indicate a constitutive increase in levels of the key antioxidant molecules glutathione and ascorbate in young leaves of the hyperaccumulator *S. pinnata* when compared with the secondary accumulator *S. albescens*.

Because *S. pinnata* had higher constitutive levels of both glutathione and AsA we examined the total antioxidant activity in young leaves of these two species by two different methods: ABTS and DPPH which both measure free radical scavenging capacities. These tests showed similar results: when grown without Se *S. pinnata* possessed a 1.5-fold higher radical

scavenging capacity than *S. albescens* (Figure 4C, D). However, when grown with Se no significant differences were observed between the species.

SMT protein levels and incorporation of Se into protein

Since the enzyme SMT is thought to be important for Se tolerance and hyperaccumulation in *Astragalus* hyperaccumulators by preventing non-specific incorporation of SeCys into proteins (Brown and Shrift, 1981, 1982; Neuhierl and Bock, 1996), SMT levels were compared between *S. pinnata* and *S. albescens*. Using polyclonal antibodies raised against AbSMT from *A. bisulcatus* (Fabaceae), immunoblots of leaf extracts from both *Stanleya* species clearly detected a single protein band that had the same size as the AbSMT (36.7 kD, Figure 5). Semi-quantification of the SMT protein band (Table 1) from plants of both species grown with Se indicated that *S. pinnata* had on average 7 times more SMT signal than *S. albescens* (Figure 5).

The relative Se protein incorporation coefficient (RSePIC) was then calculated, to investigate whether the SMT protein levels correlate with the incorporation of Se into total proteins. As shown in Table 2, leaves from the hyperaccumulator *S. pinnata* had a slightly higher RSePIC compared with the secondary accumulator *S. albescens*.

Selenium speciation and spatial distribution

To further investigate the underlying mechanisms associated with the enhanced Se tolerance and accumulation in *S. pinnata* we probed the distribution and chemical speciation of Se in young leaves of *S. pinnata* and *S. albescens* using micro X-Ray Fluorescence (μ–XRF) and X-ray Absorption Near Edge Structure (XANES). In *S. pinnata* leaves 99% of total Se was detected in organic forms corresponding with standards containing carbon-Se-carbon bonds (Table 3). In *S. pinnata* these forms were previously found using radioautography to be 83% MeSeCys and 17% selenocystathionine (SeCyst) (Shrift and Virupaksha, 1965). We later re-confirmed this result using liquid chromatography mass spectrometry (LCMS) and found a similar 80/20 percent ratio of MeSeCys and SeCyst in *S. pinnata*, respectively (Freeman et al., 2006a). The XANES spectra of Se in *S. albescens* were different and fitted best with a composition of 75% of a carbon-Se-carbon compound, 20% selenocysteine (SeCys) and 5% selenate (Table 3). Using LCMS, we further investigated the chemical composition of the free organic Se pool in *S. albescens* and found that in both young and old leaves the total free detectable organic Se pool in *S. albescens* was entirely selenocystathionine (SeCyst) with no other forms detected (Supplemental Figure 5. Together, this indicates that the total Se composition in young leaves of the secondary

accumulator *S. albescens* was 75% C-Se-C, 20% SeCys, and 5% selenate, with the free organic Se being found as SeCyst, the only C-Se-C compound detected. Since research has shown that as *A. bisulcatus* leaves age, Se speciation changes from mostly the carbon-Se-carbon form MeSeCys, to selenate (Pickering et al., 2000, 2003b), we also analyzed the Se speciation of *S. pinnata* leaves of different ages. The Se speciation in old *S. pinnata* leaves did not change and was largely the same as it was in young leaves (Table 3).

In order to compare the localization of Se in young leaves of *S. pinnata* and *S. albescens*, we used μ–XRF. Figure 6A and B show a map of total Se (in red) and Ca (in blue). Similar to what we found under different laboratory growth conditions and in the field (Freeman et al., 2006a) the *S. pinnata* young leaf accumulated Se in distinct globular areas particularly near the leaf margins and tip (Figure 6A). In contrast, the distribution of Se in *S. albescens* was diffuse throughout the entire leaf edge, and not localized in discrete areas (Figure 6B). Therefore, the hyperaccumulator *S. pinnata* and the secondary accumulator *S. albescens* showed markedly different Se speciation in their leaves, as well as different tissue Se sequestration patterns.

To investigate the localization of Se in more detail at the cellular and subcellular level we used energy dispersive spectroscopy (EDS) which determines the location of Se at a higher magnification than μ-XRF, but with lower sensitivity. This technique uses a scanning electron microscope (SEM) and EDS to probe freeze-fractured, flash frozen, fully hydrated leaves for their Se distribution. In *S. pinnata* leaves Se was detected in all epidermal cells tested and these levels decreased in epidermal cells closer to the mid-vein (Figure 6C, E). In *S. albescens* there was only one enlarged peripheral epidermal cell that showed a slightly detectable signal for Se (Figure 6D). No Se was detected in vascular or mesophyll tissues of *S. pinnata*. In a particular epidermal cell of *S. pinnata* the highest concentrations of Se were located in an organelle resembling a small vacuole (top left) (Figure 6F). The epidermal cell wall of *S. pinnata* was also tested and no Se was detected (Figure 6G). A line scan with energy insufficient to penetrate through the leaf cuticle was taken across the leaf surface and a rupture revealed the edge of a Se-rich epidermal cell immediately beneath the cuticle, indicating that Se was not accumulated in the cuticular layer (Figure 6H). Selenium was also not detected in any of the cuticular wax crystals tested. A few leaf hairs were found on field samples and in another *S. pinnata* accession; however no Se was detected in these leaf hairs (not shown). Thus, *S. pinnata* appears to sequester most Se in the symplast (perhaps in small vacuoles) of epidermal cells, and particularly in cells near the margins and tips of leaves.

Gene expression analyses

Genetic similarity test - Based on sequence identity of the internal transcribed spacer (ITS) regions 1, ITS2 and the 5.8S ribosomal RNA gene, *S. pinnata* (Gene Bank accession AF531620) is 83% identical to the Brassicaceae model species *A. thaliana* (pers. comm. W.A. Peer and D.E. Salt). In order to test whether *S. pinnata* and *S. albescens* show an equal degree of similarity to *A. thaliana*, which would make it possible to use *A. thaliana* macroarrays to compare gene expression patterns in the two *Stanleya* species, we sequenced PCR products obtained from *S. pinnata* and *S. albescens* and compared the sequences with those of *A. thaliana*. Seven independent genes, all involved in sulfur-uptake or –assimilation, were selected for the analysis (see Supplemental Table 6) because expression of these genes was expected to differ between the two *Stanleya* species. After BLAST alignment the average genetic similarity was calculated from the 7 different gene sequences (Supplemental Table 6). *S. pinnata* and *S. albescens* were on average 88 ± 2% and 89 ± 2% identical to *A. thaliana*, respectively, and 94 ± 2% identical to each other based on DNA sequence alignments. In view of the equal genetic similarity of the two *Stanleya* species to *A. thaliana* and the high cDNA sequence identity to each other we decided to use *A. thaliana* macroarrays to compare gene expression profiles in these two *Stanleya species.*

Experimental design - Sets of custom Arabidopsis cDNAs containing 324 different *A. thaliana* genes potentially involved with Se tolerance or hyperaccumulation were manually spotted onto nylon membranes (Tamaoki et al., 2008a) and hybridized with root or shoot cDNA obtained from *S. pinnata* or *S. albescens* plants treated with or without Se. Genes that showed a $\geq$2 fold higher expression level in young leaves and roots of *S. pinnata* compared to *S. albescens* grown with and without Se are listed in Table 4. Since these *Stanleya* genes have not yet been named we will refer to the genes that show differential expression in the two *Stanleya* species by the names of the *A. thaliana* cDNAs with which they hybridized on the macroarrays. Genes whose mRNA level was higher in leaves of *S. pinnata* than *S. albescens* are organized into functional groups and summarized in supplemental Figure 3. Genes that were induced by Se in both species are also provided in supplemental Tables 1, 2 and 3. Below we present the differences in gene expression between the *Stanleya* species organized by functional group.

Genes involved in sulfur/selenium metabolism – Since S and Se are thought to be metabolized by the same pathways, we compared the expression levels of S-associated genes between the two *Stanleya* species. In leaves of *S. pinnata* grown without Se four S-assimilation related genes were more highly expressed compared to *S. albescens*; three are cysteine synthase encoding genes and one a myo-inositol monophosphatase-like gene which is thought to be involved with S metabolic processes and/or histidine biosynthesis (Table 4A). In roots of *S. pinnata* grown without Se 22 different S-assimilation genes were more highly expressed compared to *S.*

albescens (Table 4B), including sulfate transporter genes, sulfate activation and reduction genes, genes mediating cysteine and methionine synthesis, and glutathione synthesis genes.

In leaves of plants grown with Se there was higher expression of 17 S-assimilation genes in *S. pinnata* compared to *S. albescens* (Table 4C), responsible for sulfate transport, sulfate reduction, sulfite reduction, and cysteine synthesis. In roots of Se-treated plants, ten S assimilation-related genes showed higher expression in *S. pinnata* compared to *S. albescens* (Table 4D), involved in sulfate transport, sulfate reduction, cysteine and methionine synthesis.

Plants have not been shown to have Se-specific enzymes, but they have Se-binding protein (SBP)-like genes. In roots of plants grown without Se a higher level of expression was observed in *S. pinnata* than *S. albescens* for two SBP-like genes: *MZN1*.9 and *SFP* (Table 4B). In leaves of plants grown with Se *S. pinnata* again showed a higher level of gene expression than *S. albescens* for two SBP-like genes, *SFP* and *SBP* (Table 4C).

Molecular chaperones and cofactor assembly genes - We examined the expression of molecular chaperone genes because they are associated with the response to various abiotic stresses and are crucial for helping proteins fold under adverse conditions. In plants grown in the absence of Se two molecular chaperone genes (*BiP1* and *BiP2*) were more highly expressed in *S. pinnata* compared to *S. albescens* (Table 4A). In roots of plants grown without Se, a higher level of expression was observed in *S. pinnata* for two heat shock protein (HSP) genes (Table 4B). In leaves of plants grown with selenate, *S. pinnata* showed a higher expression than *S. albescens* for three genes encoding HSP (Table 4C). In the roots of Se-supplied plants, the transcript levels of two HSP were higher in *S. pinnata* compared to *S. albescens* (Table 4D).

We examined the expression of genes related to biosynthesis of iron-sulfur (FeS) clusters and molybdenum cofactor (Moco) because these cofactors are associated with many important processes that may be needed for coping with Se stress. In the absence of Se no gene expression differences were observed for these genes in the leaves of *S. pinnata* compared to *S. albescens* (Table 4A). However, in roots of plants grown without Se, a higher-level of gene expression was observed in *S. pinnata* compared to *S. albescens* for six genes (Table 4B), including Cys desulfurases, activators of Cys desulfurases and various scaffold proteins for FeS assembly. When plants were grown with selenate, the expression of six cofactor-assembly genes was higher in leaves of *S. pinnata* versus *S. albescens* (Table 4C), encoding a Cys desulfurase, a Cys desulfurase activator, several FeS scaffold proteins and molybdopterin synthase sulphurylase. Two FeS cluster containing proteins were also more highly expressed (*TIC55*, *ATXDH1*). In roots of plants grown with selenate, the expression levels of three FeS scaffold encoding genes

were higher in *S. pinnata* compared to *S. albescens*, as well as five genes encoding FeS cluster containing proteins (*TIC55,* SIRB, PsaC, *PSAA*, *RDH2*).

Antioxidant and redox control genes - Because *S. pinnata* had higher antioxidant levels and radical scavenging capacities than *S. albescens* and because Se generated more oxidative stress in leaves of *S. albescens* than in *S. pinnata* leaves, we also examined the expression of antioxidant and redox control genes. In leaves of plants grown without Se, five antioxidant or redox control genes were more highly expressed in *S. pinnata* than in *S. albescens* (Table 4A), encoding a glutathione-*S*-transferase, two glutaredoxins, a catalase and a dehydro-ascorbate reductase. In roots of plants grown without Se five different antioxidant or redox control genes had higher expression in *S. pinnata* than in *S. albescens* (Table 4B), encoding a ferredoxin, two glutaredoxins, a glutathione peroxidase and an L-galactose-1-phosphate phosphatase. In Se-supplied plants eight genes encoding antioxidant or redox control enzymes showed higher expression in leaves of *S. pinnata* versus *S. albescens* (Table 4C), encoding a glutathione-*S*-transferase, two catalases, a GDP-D-mannose pyrophosphorylase, a ferredoxin, a glutathione peroxidase, a glutaredoxin and an ATP-dependent peroxidase. In roots of plants grown with Se *S. pinnata* showed higher expression levels than *S. albescens* for seven antioxidant and redox control genes (Table 4D), encoding several glutaredoxins, a ferredoxin and a glutathione reductase.

Defense-associated genes - Expression of eight defense-related genes was higher in young leaves of *S. pinnata* than in *S. albescens* when grown without selenate (Table 4A), encoding a plant defensin, *PDF1.2* (this gene showed the largest difference in expression level between *S. pinnata* and *S. albescens* of all genes tested), four pathogenesis-related (PR) proteins, a proteinase inhibitor 2 (Pin2), 1-amino-cyclopropane-1-carboxylate (ACC) synthase 6 (ACS6, involved in ethylene synthesis) and a vegetative storage protein 1 (VSP1). Five of these genes were also expressed at a higher basal level in the roots of *S. pinnata* than in *S. albescens* (*Pin2, PR1* and *5, VSP1* and *ACS6)* (Table 4B). In leaves of plants grown with Se the expression of eleven defense-related genes were higher in *S. pinnata* than *S. albescens* (Table 4C), including five of the genes also upregulated in leaves of plants grown without Se (*PDF1.2*, *Pin2*, *PR1*, *ACS6* and *VSP*1). In roots of plants grown with Se the expression of seven defense-related genes was higher in *S. pinnata* than *S. albescens* (Table 4D), including *ACS6* and *Pin2.*

Verification of gene expression patterns using Northern blotting and RT-PCR - To verify the gene expression patterns found in the macroarray studies with an independent experimental

approach and biological replicate, northern blot analysis and semi-quantitative RT-PCR was performed for selected genes. Consistent with the macroarray data, the basal expression level of defense-associated genes, *Pin2*, *PDF1.2*, and *ACS6*, was higher in *S. pinnata* than in *S. albescens* when grown without selenate (Supplemental Figure 4A, B). Moreover, the expression levels of S-associated genes, cysteine synthases, SAT52, SAT1, APS, GSH1 and GSH2, were constitutive in *S. pinnata*. Together the results from the macroarray, northern blot analysis and semi-quantitative RT-PCR approaches indicate that the expression of several key genes involved in S-uptake, -assimilation, and defense are more enhanced in *S. pinnata* than in *S. albescens*.

Tissue levels of signaling molecules and total phenolics

Because the gene expression analyses showed differences in constitutive (-Se) and inducible (+Se) expression levels of genes associated with biosynthesis of, or response to phytohormones such as methyl jasmonic acid (MeJA), jasmonic acid (JA), ethylene and salicylic acid (SA) (Table 4), we measured the plant concentrations of these hormones in young leaves of both species grown with or without Se. In addition, we measured the levels of the JA precursor methyl-linolenic acid (MeLin) in the same young leaves. When grown without Se, Me-Lin concentration was 4.5-fold higher in *S. pinnata* than in *S. albescens* ($P < 0.05$, Figure 7A), but in the presence of Se no significant difference was observed in MeLin concentrations between both species. As for JA, in the absence of Se *S. pinnata* leaves had 420 ± 137 nmol g^{-1} FW JA, while *S. albescens* did not contain any detectable JA (Figure 7B). In contrast, when grown with Se, *S. pinnata* JA levels were not detectable in young leaves while in *S. albescens* JA was present at a very low level (12 ± 8 nmol g^{-1} FW). MeJA, which is thought to be a highly bio-active hormone, was found in *S. pinnata* young leaves grown without Se at 59 ± 13 nmol g^{-1} FW while it was barely detectable (< 1 nmol g^{-1} FW) in *S. albescens* grown without Se (Figure 7C). In the presence of Se, *S. pinnata* young leaves had 3.7-fold more MeJA than *S. albescens* leaves ($P < 0.05$), with levels of 41 ± 8 and 11 ± 3, nmol g^{-1} FW, respectively.

As for the phytohormone ethylene, we found that in whole young plants of *S. pinnata* grown without Se ethylene production was 1.6-fold lower than in *S. albescens* ($P < 0.05$, Figure 7D). In contrast, in whole young plants grown with Se *S. pinnata* produced 1.6 times more ethylene than *S. albescens* ($P < 0.05$). We also measured levels of the signaling molecule SA and found that in young leaves grown without Se the concentration of free SA was 10.8 times higher in *S. pinnata* than in *S. albescens* (Figure 7E). When grown with Se the levels of SA in *S. pinnata* young leaves were 4.6 fold higher than *S. albescens* ($P < 0.05$).

Finally, total phenolics (TP) were measured in the young leaves. Phenolic compounds are often associated with abiotic stress defense and signaling disease resistance and are considered a good indicator of the antioxidant capacity of leaves. We found that in plants grown without Se the TP levels of *S. pinnata* were 1.6-fold higher compared to *S. albescens* (Figure 7F), and in plants grown with Se the *S. pinnata* TP levels were 1.3-fold higher than *S. albescens* ($P < 0.05$).

Thus, in comparison with the secondary accumulator *S. albescens*, the hyperaccumulator *S. pinnata* showed a trend for higher levels of JA, its precursor MeLin and active derivative MeJA, as well as higher SA and total phenolics. Ethylene in whole young plants showed mixed results. In the absence of Se it was present at lower levels in *S. pinnata*, but it appeared to be induced more strongly by Se in the hyperaccumulator, so that its level was higher in *S. pinnata* than in *S. albescens* whole young plants when grown in the presence of selenate.

Physiological effects of MeJA, ACC and OAS on Se accumulation in shoots

To obtain further insight into the effects of the phytohormones and signaling molecules measured previously on shoot Se accumulation, we applied these compounds as foliar spray treatments to the shoots of young plants. MeJA at 10 μM was effective at increasing Se accumulation in both *S. pinnata* and *S. albescens* shoots (Figure 8A). Six-week old plants of *S. pinnata* grown in the presence of 20 μM selenate that had been sprayed daily with 10 μM MeJA during the last three weeks had accumulated 1.6-fold more Se than water controls ($P < 0.05$). Similarly, *S. albescens* accumulated 2.8-fold more Se after 10 μM MeJA treatment compared to water controls ($P < 0.05$). At 100 μM MeJA both species did not accumulate more Se than water controls.

1-amino-cyclopropane-1-carboxylate (ACC) is an ethylene precursor often used in ethylene elicitor experiments. Spraying young *S. pinnata* shoots with 10 μM ACC every day for three weeks did not significantly affect shoot Se accumulation compared to water controls (Figure 8B). However, *S. albescens* accumulated 2-fold more Se compared to its water control when 10 μM ACC was applied ($P < 0.05$). At the 100 μM ACC treatment level both species did not accumulate more Se than their water controls and the plants were smaller in size indicating inhibition of growth at this ACC concentration.

Because of the expression differences observed between *S. pinnata* and *S. albescens* with respect to genes involved in sulfur transport and assimilation we tested the effect of treatment with O-acetylserine (OAS) on the ability of both species to accumulate Se. It is known that OAS, the carbon substrate for cysteine biosynthesis, up-regulates the key genes involved in

sulfur transport, reduction and assimilation. After 30 days of growth in media containing 20 μM selenate but no OAS (Figure 8C), the Se accumulation in *S. pinnata* young shoots was 1.5-fold higher than in *S. albescens* ($P < 0.05$). After growth in media containing both 20 μM SeO_4^{2-} and 50 μM OAS, *S. pinnata* had accumulated 1.4-fold more Se than its control grown without OAS ($P < 0.05$), while *S. albescens* accumulation was not affected by the same treatment. At 100 μM OAS *S. pinnata* had accumulated marginally more Se than its control grown without OAS. However, *S. albescens* young shoots showed a decrease in Se content by 2.4-fold compared to its control grown without OAS ($P < 0.05$). Thus, OAS stimulated Se accumulation in *S. pinnata* young shoots but not in *S. albescens*.

Discussion

The data presented in this manuscript provide new insight into Se tolerance and sequestration mechanisms in the Se hyperaccumulator *S. pinnata*. These data are novel, since earlier work on Se tolerance and accumulation mechanisms have mainly been performed on hyperaccumulator *A. bisulcatus*, the secondary accumulator *B. juncea*, and the non-accumulator *A. thaliana*. Some of the mechanisms proposed here for *S. pinnata* appear to be different compared to *A. bisulcatus* (e.g. with respect to upregulation of S assimilation genes), but there are also interesting parallels (e.g. the main form of free Se accumulated and the preferential accumulation in the epidermis). This manuscript also describes the first transcriptome analysis of any Se hyperaccumulator and identifies new genes that may contribute to the Se hyperaccumulation phenotype of the Brassicaceae family member *S. pinnata*.

Hyperaccumulator *S. pinnata* was completely tolerant to 20μM selenate, while *S. albescens* suffered toxicity at this concentration, judged from visible leaf chlorosis and necrosis, accumulation of ROS, and decreased photosynthetic performance. Shoot Se accumulation was ~3.6-fold higher in *S. pinnata*, demonstrating that the enhanced Se tolerance of *S. pinnata* is due to detoxification and not exclusion. Our biochemical studies offer some insight into the molecular mechanisms potentially mediating these differences in Se tolerance and accumulation. One important molecular mechanism for Se tolerance in *S. pinnata* is likely the chemical form into which inorganic Se is converted and then hyperaccumulated. The free Se in young leaves of *S. pinnata* consists of ~80% MeSeCys and ~20% selenocystathionine, with no detectable inorganic forms as judged from LCMS; similarly, XANES Se analysis of *S. pinnata* found greater than 98% of Se as C-Se-C forms (Shrift and Virupaksha, 1965; Freeman et al., 2006, this study). In contrast, the secondary accumulator *S. albescens* contained only selenocystathionine

as the detectable free organic Se form in both young and old leaves as judged from LCMS. XANES Se speciation analysis demonstrated for *S. albescens* that C-Se-C forms represented 75% of total Se, along with 20% selenocysteine and 5% selenate. The high MeSeCys levels in *S. pinnata* may be explained by its increased level of SMT protein, which was detected on average 7-fold more than in *S. albescens* in immunoblotting. Accumulation of Se as MeSeCys is thought to offer a safe way to sequester Se, since this amino acid does not get misincorporated into proteins, and thus likely contributes to the enhanced Se tolerance and hyperaccumulation of *S. pinnata* (Brown and Shrift, 1981, 1982; Neuhierl and Bock, 1996). While the only free organic form found in *S. albescens*, selenocystathionine, may offer some protection from Se incorporation into protein it may be more toxic than MeSeCys. Selenocystathionine is a minor constituent of total Se in hyperaccumulators while MeSeCys is usually the predominant form in hyperaccumulators. Moreover, species such as *A. bisulcatus* or *A. racemosus* with the highest Se hyperaccumulation (5,000 – 10,000 μg total Se g^{-1} DW) typically contain exclusively MeSeCys, while species such as *S. pinnata, Neptunia amplexicaulis* and *A. pectinatus*, which show less extreme Se hyperaccumulation (2,000 – 5,000 μg total Se g^{-1} DW) typically contain a mixture of 70-80% MeSeCys and 20-30% SeCyst, (Shrift and Virupaksha 1964, Freeman et al 2006, Peterson and Butler 1967, Horn and Jones 1941). Species such as the Se accumulator *Morinda reticulata* that accumulate ~90% of total Se as SeCyst closely match the secondary accumulator *S. albescens* in their total Se accumulation when fed Se (Peterson and Butler 1971). Moreover, SeCyst is a metabolic intermediate between SeCys and SeMet, and both amino acids can be toxic to plants when incorporated into protein (reviewed by Pickering et al., 2003b). MeSeCys, on the other hand, is the result of a branching pathway that moves Se away from incorporation into protein. It is possible that the SeCyst accumulation found in both *S. pinnata* and *S. albescens* offers some protection from Se incorporation into proteins in the form of SeMet, but may not protect against SeCys being misincorporated into protein, which likely is more toxic than SeMet misincorporation in view of the important functions of Cys residues in disulfide bonds often required for proper protein structure and function. The selenocysteine and selenate found to make up the additional 25% of total Se in *S. albescens* are more toxic than MeSeCys or SeCysth, and most likely further contribute to toxicity. Incidentally, it is interesting that this secondary accumulator, *S. albescens*, accumulated such a large fraction of Se in organic form. Other secondary accumulators and non-accumulators were reported to accumulate mainly selenate when supplied with selenate, with a minor fraction of organic Se with a XANES spectrum similar to SeMet (de Souza et al., 1998; Van Hoewyk et al., 2005). These results however may be artifactual and completely due to the short time after selenate treatment before these plants

were harvested. Based on XANES alone SeMet, MeSeCys and SeCyst cannot be distinguished (all contain C-Se-C) and thus it is possible that this minor organic fraction was SeCysth. Mass spectrometry studies did indeed reveal the presence of SeCyst in *B. juncea, Lecythis minor and A. thaliana*, all secondary accumulators or non-accumulator plants (Montes-Bayon et al., 2002, Dernovics et al., 2007).

It is surprising that hyperaccumulator *S. pinnata* did not show a lower level of Se incorporation into protein than the non-accumulator *S. albescens*. For comparison, Se incorporation into protein in the hyperaccumulator *Astragalus bisulcatus* was lower than in non-accumulator *A. drummondii* (values were 0.09 ± 0.015 and 0.343 ± 0.097 Se $\mu g\ g^{-1}$ total protein divided by leaf Se $\mu g\ g^{-1}$DW, respectively). Despite their similar levels of Se incorporation into total protein, *S. pinnata* accumulated 3.6-fold more Se and did not suffer any Se toxicity while *S. albescens* clearly did. This could suggest that the observed Se toxicity is also due to some other process than Se incorporation into protein (e.g. oxidative stress caused by inorganic Se), or that Se incorporation in *S. pinnata* proteins happens in less harmful aminoacids (SeMet rather than SeCys) or proteins, or in a more regulated manner than in *S. albescens*. Past bioinformatic analysis has not revealed any essential selenoproteins in higher plants (no SeCys insertion sequence has been found; Stillwell and Berry, 2005; Zhang and Gladyshev, 2009), but it cannot be excluded that Se is incorporated post-translationally into some proteins, e.g. by modifying a serine residue to a SeCys enzymatically. In this context, it is interesting to note the early report by Shrift and Virupaksha (1965) that *S. pinnata* showed a minor Se-enriched radioactive band with an R_f greater than glutathione. When this band was hydrolyzed with 4N HCl, chromatography showed several ninhydrin-positive spots with small amounts of radioactivity being present at the position of SeCys. These results first indicated that *S. pinnata* has a peptide which contains SeCys and other amino acids (Shrift and Virupaksha, 1965). Also interesting to note is that the gene that showed the biggest upregulation in *S. pinnata*, *PDF1.2*, encodes a small and extremely Cys-rich pathogen defensin protein (Broekaert et al., 1995; Penninckx et al., 1996). Overproduction of a similar plant defensin from the Zn hyperaccumulator *Arabidopsis halleri* (*AhPDF1.1*) in *A. thaliana* led to a significant increase in resistance to Zn and selenite (Mirouze et al., 2006; Tamaoki et al., 2008b). Considering the known role for Se in *S. pinnata* elemental defense (for a review see Quinn et al., 2007), one may envision the presence of a SeCys-rich toxic defense protein. Misincorporation rates alone for SeCys into highly expressed Cys-rich PDF protein in the hyperaccumulator plant may contribute to enhanced elemental defense and Se tolerance. It can also be hypothesized that Se is bound by particular *S. pinnata* proteins rather than being present in the primary protein sequence as SeCys. Our macroarray

results did show evidence of increased expression of two Se-binding protein (SBP) encoding genes, but whether the Se bound by such a protein would still be present after TCA precipitation and acetone wash is questionable.

The tolerance of *S. pinnata* to Se may also involve the sequestration of Se in specific epidermal locations. XRF mapping showed that in *S. pinnata* Se was accumulated in discrete "hot spots" along the leaf margins, while in *S. albescens* the distribution of Se was diffuse throughout the leaf. EDS showed Se levels to be highest in *S. pinnata* epidermal cells around the leaf edges, with decreasing epidermal Se concentrations closer to the mid-vein. No Se was detected in vascular, spongy parenchyma or palisade parenchyma cells of *S. pinnata*, suggesting the *S. pinnata* peripheral epidermal cell clusters are the predominant sites of Se sequestration. In *S. albescens* EDS only detected Se in one single, epidermal cell. Inside *S. pinnata* epidermal cells the highest concentrations of Se were present in an organelle that resembles a small vacuole. The cell walls of *S. pinnata* had no detectable Se. Selenium was not detected in the cuticle, or in any cuticular wax crystals tested. This is noteworthy because an earlier finding reported a potential seleniferous leaf wax in *S. bipinnata* (McColloch et al., 1963). No Se was detected in leaf hairs, the predominant site of sequestration in another hyperaccumulator, *A. bisulcatus* (Freeman et al., 2006). Thus, *S. pinnata* appears to sequester most of its Se in the symplast, in small vacuoles of epidermal cells, particularly near the leaf edges. The unique Se transport and sequestration mechanisms into and out of these localized cells is unknown and deserves further exploration as one of the possible key mechanisms for Se hypertolerance and hyperaccumulation. It is possible that Se accumulation in localized areas both prevents plants from Se toxicity and provides a storage mechanism for organic non-toxic Se to remobilize for future biotic defense in growing young leaves and reproductive parts.

Another mechanism contributing to *S. pinnata*'s Se tolerance may be its capacity to prevent or reduce Se-associated oxidative stress. The decreased photosynthetic performance in Se-treated *S. albescens* may have been caused by Se-induced problems with the photosynthetic machinery, either via selenate-mediated oxidative stress or via replacement of sulfur amino acids by their Se analogs in photosynthetic proteins. Such negative effects of Se on photosynthesis may be further magnified by a subsequent increase in ROS generation. Electrons lost from inefficient photosynthetic electron transport can react with molecular oxygen, forming superoxide which then is converted to hydrogen peroxide and other free radical intermediates. Visualization of ROS *in situ* using hydrogen peroxide- or superoxide-sensitive dyes showed that *S. pinnata* accumulated lower levels of ROS than *S. albescens*. Prolonged exposure to ROS may have caused a programmed cell death (PCD) cascade in *S. albescens* leaves, leading to the

observed chlorosis and necrotic lesions. Leaves of *S. pinnata* contained higher levels of the ROS scavenging metabolites GSH and AsA compared to *S. albescens* leaves, suggesting a higher free radical scavenging capacity that would explain the observed lower levels of ROS accumulation in *S. pinnata* in the presence of Se. The high level of GSSG in *S. pinnata* suggests that ROS were generated in this hyperaccumulator, but that the increased glutathione pool was potentially able to better scavenge the Se-associated free radicals before they could cause oxidative stress. Our previous study with non-hyperaccumulator *A. thaliana* indicated that an optimal level of ROS generation is necessary for selenite resistance in this species (Tamaoki et al., 2008a). We hypothesized that ROS production in *A. thaliana* may be required as signal molecules for activation of pathways that lead to Se resistance. In analogy, it is possible that 20 μM Se treatment leads to optimal ROS levels for Se tolerance in *S. pinnata*, while in *S. albescens* this same Se treatment leads to excess levels of ROS, damaging photosystems and triggering PCD pathways.

Perhaps further lowering oxidative stress, *S. pinnata* showed higher expression levels of several molecular chaperone encoding genes (luminal binding proteins, heat shock proteins). Enhanced expression level of molecular chaperones may contribute to *S. pinnata*'s capacity to prevent oxidative stress, by helping repair any Se-induced problems with protein folding or stability. Moreover, there was a trend for genes involved in the biosynthesis of FeS clusters or MoCo to be more highly expressed in *S. pinnata* compared to *S. albescens*; a similar pattern was observed for the expression levels of several genes encoding proteins that require these cofactors to function. Since FeS clusters and MoCo are sensitive to oxidative stress, and the absence of the cofactor usually leads to degradation of the cofactor-requiring protein, the upregulation of these genes results may reflect a better capacity in the hyperaccumulator to reconstitute these cofactors, which may in turn explain their better photosynthetic capacity.

Stanleya pinnata showed constitutive up-regulation of genes involved in biosynthesis of the phytohormones MeJA, JA, SA and ethylene. These hormones are typically associated with stress and defense responses in plants. JA and ethylene were shown earlier to also be involved in selenite resistance in *A. thaliana* (Tamaoki et al, 2008a). A more Se-resistant accession of this species produced higher levels of JA and ethylene in response to Se treatment, and genes involved in the synthesis of these hormones were more highly induced. Moreover, knockout mutants unable to synthesize or respond to these hormones showed reduced resistance, while supply of the hormones to a more Se-sensitive accession enhanced resistance. We hypothesized that the positive effects of these hormones on Se tolerance may be due to upregulation of S uptake and assimilation. MeJA has been shown to upregulate genes involved in primary and

secondary S-related pathways (Jost et al., 2005). After selenite treatment genes encoding key reactions of sulfate assimilation and glutathione synthesis were indeed upregulated in *A. thaliana* (Tamaoki et al., 2008a). Constitutive upregulation of S assimilation may enable the plant to more efficiently prevent Se analogs from replacing S in proteins and other S compounds.

In *S. pinnata*, many important S assimilation pathway genes were found to be constitutively upregulated compared to *S. albescens*. The constitutively upregulated sulfate/selenate assimilation pathway in roots and shoots may explain the higher total S and Se levels in the hyperaccumulator, as well as the higher levels of reduced antioxidant thiols. When grown with Se, *S. pinnata* had accumulated 1.3-fold more S than *S. albescens* and mature leaves of *S. pinnata* plants with Se contained 60% higher non-protein thiol levels compared to the mature leaves of *S. albescens*. When grown with Se *S. pinnata* contained a 1.4-fold higher level of GSH, a 1.2-fold higher GSSG level and a 1.3-fold higher total glutathione level than *S. albescens*. In the Se-sensitive species *S. albescens* there was a significant drop in the reduction state of its glutathione pool when treated with Se while in the Se-tolerant *S. pinnata* the ratio of reduced to oxidized glutathione was unchanged. It is highly plausible that part of the Se tolerance mechanism in *S. pinnata* is its ability to prevent sulfur starvation in the presence of Se and that *S.albescens* is suffering from sulfur deficiency when grown with Se.

The genetic mechanisms likely responsible for the increased Se and S accumulation ability of the Se hyperaccumulator *S. pinnata* are also discovered herein because in *S. pinnata* leaves grown without Se three cysteine synthase genes were constitutively upregulated (Fig 4A). In roots of *S. pinnata* grown without Se 22 different S-assimilation genes were more highly expressed compared to *S. albescens* (Table 4B). These included a sulfate transporter gene Sultr1;2 previously shown to result in selenate resistance in *A. thaliana* when knocked out (Shibagaki et al., 2002). This implicates Sultr1;2 in the non-specific transport of selenate into *A. thaliana* roots; perhaps a homologue in *S. pinnata* has evolved to function mainly in selenate uptake. In this context it is interesting that the Se/S ratio, a direct μg comparison, was 0.43 for *S. pinnata* and 0.19 for *S. albescens*, while the selenate/sulfate ratio in the supplied medium was 0.05. The hyperaccumulator had both higher S and Se levels than the non-hyperaccumulator, but appeared to have a higher preference for Se relative to S. This is in support of the presence of a specialized selenate transporter in the hyperaccumulator. A high Se/S ratio is thought to be one of the typical characteristics of hyperaccumulators (White et al., 2004, 2007). In agreement with our observed constitutive upregulation of genes responding to MeJA-, JA- and SA-signaling in *S. pinnata*, the levels of these hormones were constitutively higher in the hyperaccumulator leaves and they were induced in response to Se in *S. albescens* roots. External supply of MeJA or ACC

resulted in enhanced levels of Se accumulation in *S. albescen*s over this short-term experiment. These results indicate that internal MeJA and/or ethylene levels cause a higher Se accumulation capacity in *Stanleya* species, with hyperaccumulators having higher constitutive levels of these hormones than non-hyperaccumulators. Taken together, constitutive upregulation of S assimilation mechanisms, mediated by MeJA, JA and/or SA may be an important underlying molecular mechanism for *S. pinnata*'s Se tolerance and hyperaccumulation.

The same hormones, MeJA, JA and SA, function to upregulate defense-associated genes when plants are attacked by pathogens or herbivores (Wang et al., 2002; Turner et al., 2002; Durrant and Dong, 2004). Thus, it is not surprising that *S. pinnata* showed constitutive upregulation of many defense-associated genes, including the Cys-rich PDF gene mentioned above. Whether the upregulation of this class of genes plays any role in Se tolerance or accumulation is at this point unclear. The upstream signal transduction changes that constitutively upregulate S assimilation (via MeJA, JA, SA, ethylene) may simply also turn on these defense-related genes, without having an additional effect on Se metabolism. Alternatively, it is possible that these genes, traditionally associated with biotic stress resistance, also serve functions in abiotic stress resistance and are regulated by the relative oxidative status of the plant. ROS-antioxidant interaction is inherently involved in many different stresses and responses of plants to their environment (Foyer and Noctor, 2005). An elemental stimulus such as Se that disrupts cellular redox balance could serve as an inducer for sets of defense-related genes including PR proteins. Low levels of ascorbate and changes in the cellular glutathione pool can also elicit pathogen resistance responses (Pastori et al., 2003; Barth et al., 2004; Mou et al., 2003; Gomez et al., 2004).

Earlier studies have particularly focused on the Se hyperaccumulator *Astragalus* and on SMT as a key enzyme for Se hyperaccumulation and tolerance (Neuhierl and Bock, 1996; Ellis et al., 1996; Sors et al., 2005, 2009). Comparative *Astragalus* studies found a correlation between hyperaccumulation and SMT but no difference in the enzymatic rates of S assimilation between various hyperaccumulator and non-accumulator species (Sors et al., 2006). In *S. pinnata*, SMT protein levels were also elevated compared to the non-hyperaccumulator. This likely constitutes one of the underlying mechanisms for the Se tolerance and hyperaccumulation in this species since the main form of Se accumulated in *S. pinnata* is methyl-SeCys, while in the non-hyperaccumulator it is Se-cystathionine. However, the elevated SMT appears to be but one piece of the puzzle controlling Se hyperaccumulation. Sequestration of MeSeCys in the vacuoles of specialized epidermal cells may be another. Moreover, it appears that the S assimilation pathway is constitutively upregulated in the *S. pinnata* hyperaccumulator, judged from the higher levels of

transcripts observed and the higher total S and GSH levels. The enhanced transcript levels of genes involved in S-assimilation in *S. pinnata* compared to *S. albescens*, particularly in the absence of Se and in the roots, indicate that the expression of these genes is constitutively upregulated in the Se-hyperaccumulator *S. pinnata*. The expression of similar genes was also frequently induced by Se in the non-hyperaccumulator *S. albescens*. It may be proposed that *S. pinnata* has lost the ability to sense its overall S status and behaves as if it is continuously S-starved. This in turn may affect cellular redox state, S and Se levels and thus Se hyperaccumulation. The upregulated S assimilation pathway may alleviate a bottleneck for both sulfate and selenate transport followed by assimilation into Cys/SeCys, and the elevated SMT levels further convert SeCys into non-toxic MeSeCys. The key to the upregulation of these S-related pathways in *S. pinnata* appears to be controlled in part through constitutively elevated levels of the signaling molecules MeJA, JA and SA. The upstream mechanisms that result in the upregulation of these hormone levels will be an interesting topic for further study. Future, more comprehensive transcriptomic studies may reveal one or more key genes upstream to the ones observed in this study, that respond to Se and upregulate the genes causing the elevated hormone and S levels.

Identification and comparison of these key genes would open the possibility of transferring the entire Se hyperaccumulator syndrome to fast-growing non-accumulator species with favorable properties for phytoremediation or for producing Se-enriched bio-fortified food. Further research may also reveal hyperaccumulator-specific signal transduction mechanisms, Se transporters for uptake of selenate and for the transport and sequestration of other selenocompounds, particularly MeSeCys.

Materials and Methods

Plant growth

Stanleya pinnata seeds were obtained from native plants growing in the field in Pine Ridge Natural Area in West Fort Collins, Colorado. *Stanleya albescens* seeds were collected from the Uncompahgre plateau in Western Colorado.

During plant plate growth experiments plants were grown for 30 d on square agar plates containing half-strength MS salt plus B5 vitamins, with and without 40 μM selenate. Sucrose was excluded from all experiments. Seeds from *S. pinnata* and *S. albescens* were grown on separate plates to exclude any phytotoxic effects of seeds from one species to those of the other.

When growing plants to measure Se accumulation, physiology of Se toxicity, SMT immunoblot, Se protein incorporation, macroarray and metabolic analyses experiments followed an arid western plant growth protocol previously used for Se hyperaccumulators and described by Sors et al. (2005). Twenty plants per treatment from each species were grown via a controlled drip system in a sterilized, pathogen free laboratory growth room on pre-soaked and water rinsed gravel (Turface) in round 25 cm diameter pots, for 16 weeks, with and without 20 μM selenate. No sign of any pathogen infection was ever observed in these plants. They were fertilized with (in mg per L) 200 N, 29 P, 167 K, 67 Ca, 30 Mg and micronutrients. Nutrients were supplied from 1 g/L 15-5-15 commercial fertilizer formulation (Miracle Gro© Excel© Cal-Mag; The Scotts Co., Marysville, OH). Adjustment of pH to range 5.7 - 6.0 was achieved via 93% sulfuric acid at 0.08 mL/L. Next to each seedling this solution was dripped into each pot 4 times weekly, 20 mL of solution during weeks 1-5, 50 mL weeks 5-10 and 100ml weeks 10-16 for each mature plant used. Plants were grown at (24/20°C (day/night), 16-h photoperiod with a full spectrum photosynthetic photon flux density of 300 μmol m^{-2} sec^{-1}).

Leaf harvest

Young leaves from plants were harvested and flash-frozen after 10 weeks. Leaf number for all treatments and species at ten weeks were on average 11.2 ± 1.7. No visible toxicity sign of any kind was observed in leaves when they were harvested at ten weeks and a portion was stored at -80°C for genetic and biochemical analysis. Fresh leaves at ten weeks were used for *in situ* ROS tests. After 16 weeks plants were used for chlorophyll fluorescence measurements before leaves were harvested for toxicity pictures and total Se analysis.

Quantification of selenium and sulfur accumulation

Plant materials were rinsed with distilled water, and dried at 45°C for 48 h. Replicates were acid digested and analyzed for Se and S by inductively coupled plasma atomic emission spectrometry (ICP-AES) as described by Pilon-Smits *et al*. (1999).

Quantification of selenium tolerance index

For quantification of selenate resistance, plants were grown on vertically placed agar plates for 30 d with or without 40 μM selenate and root length was measured. The Se tolerance index was calculated for both species as root length grown in the presence of selenate divided by mean of

root length on control medium as described by Zhang et al. (2006) and Tamaoki et al. (2008a). Ten replicate plants were measured for each plant species and treatment.

Chlorophyll fluorescence measurements

Light intensity dependent electron transport rate was measured after 16 weeks of growth from 6 plants per treatment using the method described by Abdel-Ghany *et al.* (2005). Relative electron transport rate was calculated from the product of ΦPSII (electron flux through photosystem II) and light intensity (μmol m^{-2} s^{-1}). The resulting chlorophyll fluorescence parameter represents the efficiency of PSII photochemistry (Genty et al., 1989).

***In situ* ROS detection**

Selenium-induced *in situ* accumulation of superoxide was detected with NBT (nitro blue tetrazolium, Boehringer Mannheim, Germany) as described by Jabs et al. (1996). To visualize *in situ* accumulation of hydrogen peroxide, 3,3'-Diaminobenzidine (DAB) staining was performed as described by Torres et al. (2002).

Antioxidant analyses

To measure reduced (GSH) and oxidized (GSSG) glutathione levels, 100 mg of fresh leaves were homogenized in 2 mL of cold 5% (w/v) metaphosphoric acid. GSH and GSSG contents were measured as described by Yoshida *et al.* (2006).

For measurement of ascorbic acid (AsA) content, leaves were freeze-dried using a Genesis Freeze Drier (Virtis, Inc., Gardiner, NY). Lyophilized samples were then weighed to determine percent dry matter content and ground in preparation for extraction. The dried samples were ground into a fine powder using a mortar and pestle and sieved with a No. 20 Tyler sieve (WS Tyler Inc., Mentor, OH). For sample extraction, 5 mL of 80% acetone (Fisher Scientific, Fair Lawn, NJ) and 200 mg powder from each replicate were placed in 15 mL centrifuge tubes. The tubes were thoroughly mixed, rotated in the dark (4˚C) for 15 minutes, then centrifuged (4˚C; 4,000 rpm) for 15 minutes. One mL of supernatant fluid was transferred to a microcentrifge tube and vacufuged at 45˚C to dryness (approximately 2-3 hours). Samples were stored at -20˚C until analytical tests were completed. Ascorbic acid (vitamin C) content was determined using a high-performance liquid chromatography (HPLC) method as described Esparaza Rivera, et al. (2006) and modified from Galvis Sanchez, et al. (2003). Freeze-dried samples were extracted with a 5% w/v aqueous solution of metaphosphoric acid containing 1% w/v dithiothreitol (DTT) (Promega

Corp., Madison, WI), and then allowed to rotate for 15 minutes at 4˚ C. The samples were centrifuged for 5 minutes at 4,000 rpm and 4˚ C before the supernatant was filtered through a 0.45 µm nylon syringe filter. The extraction process was repeated and the supernatant from both extractions was placed in an amber HPLC vial. Ascorbic acid standards were made by mixing 100 mg DTT (Promega Corp.), 10 mg ascorbic acid (Sigma-Aldrich), and 10 mL of 100% methanol before diluting to five concentrations for the standard curve. All samples were analyzed by HPLC (Hewlett Packard Model 1050 Series, Palo Alto, CA) using an Inertsil C4 column run with a phosphoric acid/methanol gradient and absorbance read at 254 nm and analyzed using Chem Station for LC Rev A 09.01 software (Agilent Technologies, Palo Alto, CA).

Antioxidant capacity

Leaves were freeze-dried using a Genesis Freeze Drier (Virtis, Inc., Gardiner, NY). Lyophilized samples were then weighed to determine percent dry matter content and ground in preparation for extraction. The dried samples were ground into a fine powder using a mortar and pestle and sieved with a No. 20 Tyler sieve (WS Tyler Inc., Mentor, OH). For sample extraction, 5 mL of 80% acetone (Fisher Scientific, Fair Lawn, NJ) and 200 mg powder from each replicate were placed in 15 mL centrifuge tubes. The tubes were vortexed until thoroughly mixed, rotated in the dark (4˚ C) for 15 minutes, then centrifuged (4˚C; 4,000 rpm) for 15 minutes. One mL of supernatant was transferred to a microcentrifuge tube and vacufuged at 45˚C to dryness (approximately 2-3 hours). Samples were stored at -20˚C until analytical tests were completed.

The 2,2'-azino-bis(3-ethylbenzothiazoline-6-sulfonic acid) diammonium salt assay was used to estimate antioxidant capacity. This assay is based upon measuring the capacity of an extract to scavenge and detoxify the $ABTS^{\bullet+}$ radical and is considered an estimate of hydroxyl scavenging activity (Miller and Rice-Evans 1996). The protocol used was based on the microplate method described by Esparaza Rivera et al. (2006), as modified from Miller and Rice-Evans (1996). The $ABTS^{\bullet+}$ solution was prepared by mixing 40 mg $ABTS^{\bullet+}$ (Calbiochem, EMD Biosciences, La Jolla, CA), 15 mL distilled water, and 2.0 ± 0.5 g MnO_2 (Sigma-Aldrich). After 20 minutes, the MnO_2 was removed using double filtration, first with a vacuum filtration and second with a 0.2 µm syringe filter. The absorbance value of the $ABTS^{\bullet+}$ solution was read at 734 nm in the Spectra Max Plus (Molecular Devices, Sunnyvale, CA) spectrophotometer using Softmax Pro software (Molecular Devices) and adjusted to 0.70 absorbance units (AU) by adding 5.0 mM phosphate buffer solution. Once the $ABTS^{\bullet+}$ solution was adjusted, it was held at 30˚ C and used within 4 hours. Vacufuged samples were reconstituted with 1 mL 80% acetone (Fisher

Scientific). Twenty-five µL of each reconstituted sample was mixed with 250 µL of the $ABTS^{\bullet+}$ solution, and the absorbance value was read after exactly 60 seconds at 30 ºC in a temperature-controlled microplate reader. $ABTS^{\bullet+}$ antioxidant capacity was reported as Trolox equivalent antioxidant capacity (TEAC) per gram of sample on a fresh weight basis (TEAC/g FW) and was calculated by comparing to a Trolox (Calbiochem) standard curve. Analyses were run in triplicate at 3 dilutions for a total of 9 assays per sample.

The 2,2-diphenyl-1-picrylhydrazyl ($DPPH^+$) assay was also used to estimate antioxidant capacity and was measured using the method of Lu and Foo (2000) with some modifications. Vacufuged samples were reconstituted with 1.0 mL of 5.0 mM phosphate buffer solution. A 0.1 mM $DPPH^+$ solution was made by mixing 7.89 mg $DPPH^+$ with 100% methanol. Absorbance was read in the Spectra Max Plus (Molecular Devices, Sunnyvale, CA) spectrophotometer using Softmax Pro software (Molecular Devices) at 515 nm and adjusted to 0.95 AU. Fifteen µL of the reconstituted samples were mixed with 285 µL of the $DPPH^+$ solution, and read at 515 nm exactly after being held for three minutes at 25˚C. The results were compared to a Trolox (Calbiochem) standard curve and expressed as TEAC/100 g FW.

Western Blot

SDS-PAGE was performed according to Laemmli (1970) using 12.5 % gels. Immunoblotting experiments were carried out according to Neuhierl et al. (1999) using 30 µg of total leaf protein loaded from each plant and an anti-*A. bisulcatus* SMT antibody at a 1:4,000 dilution. Quantification of immunoreactive bands was achieved using the ImageJ program (National Institutes of Health, Bethesda, MD; http://rsb.info.nih.gov/ij). *A. bisulcatus* SMT protein was predicted from its sequence to be 36.7 KD (Neuhierl et al., 1999).

Se protein incorporation

Protein was extracted as described by Garifullina et al. (2003) and a portion was quantified by bicinchoninic acid (BCA) protein assay kit from Pierce, according to manufacture direction. Total protein concentrations were then adjusted to be equal and precipitated with trichloroacetic acid (TCA) and washed two times with Acetone. The acetone-washed total protein pellet was then acid-digested, assayed by ICP-AES, and the amount of Se in total proteins was normalized to total Se in leaves to calculate total Se protein incorporation coefficient by the method of Garifullina et al. (2003).

Se Standards

Na_2SeO_4 (S8295), Na_2SeO_3 (S1382), SeCystine (S1650), and SeMet (S3132) were obtained from Sigma-Aldrich. MeSeCys, γGMeSeCys and $SeGSH_2$ standards were obtained from PharmaSe. SeCys was obtained by reducing SeCystine at 25°C overnight in 100 mM sodium borohydride at a 1:1 molar ratio. Gray and red elemental Se were generously provided by Amy Ryser and Dan Strawn.

μ-XRF/μ-XAS

Samples were washed to remove any external Se, flash frozen in LN_2 and shipped on dry ice to the Advanced Light Source at the Lawrence Berkeley Laboratory for micro-spectroscopic analysis on Beamline 10.3.2 (Marcus et. al., 2004). The total distribution of Se was mapped by scanning the samples in the microfocused x-ray monochromatic beam at 13085 eV. Samples were mounted onto a Peltier stage kept at -33°C to reduce potential radiation damage. μ-SXRF mapping of Se was performed first on all samples. Large maps were collected using a 7 μm (horizontal) x 7 μm (vertical) beam at 13085 eV sampled in 20 μm x 20 μm pixels. The Kα fluorescence line intensities of Se (and other elements of interest) were measured with a 7 element Ge solid state detector and normalized to the incident beam intensity and dwell time. The chemical forms of Se on spots of interest in sample X were further investigated using microfocused Se K-edge XANES. XANES provides information about the oxidation state and, when compared to well-characterized Se standard compounds, information about its chemical speciation (Pickering et al., 1999). Aqueous solutions of the various selenocompounds were used as standard materials. Red Selenium (white line maximum set at 13074.73eV) was used for energy calibration. Micro-XRF and XANES data analysis was performed with a suite of LabVIEW programs (National Instruments) available at Beamline 10.3.2 (http://xraysweb.lbl.gov/uxas/Beamline/Software/Software.htm).

Energy Dispersive Spectrometry

Young leaves from mature plants of S. *pinnata* and S. *albescens* were washed to remove any external Se. They were then placed in plastic test tubes with the base of the petiole immersed in water to prevent dehydration and sealed before overnight shipping to Rothamsted Research UK. Energy Dispersive Spectrometry (EDS) was used to analyze for Se on the fully hydrated freeze fractured leaves. Leaf tissue (7 mm x 5 mm) was cut from each specimen using a sterile blade, mounted on a cryo stub using OCT compound (Sakura-Netherlands) and plunge frozen in pre-slushed LN_2. The specimen was transferred under vacuum to the GATAN Alto 2100 cryo

chamber (Gatan UK) with temperature maintained at minus 180°C. Here it was fractured, etched to remove any contaminating ice and coated with Au for examination. The specimen was then passed into the JEOL LV6360 scanning electron microscope (Jeol UK) and mounted on the stage with the temperature maintained at minus 160°C and with parameters set for EDS analysis using the OXFORD INCA 2000 microanalysis system (Oxford Instruments). The L line for Se was chosen to avoid peak interference on the Kα line and an acceleration voltage of 5,000eV.

Macroarray gene expression analysis

Expression of 324 different genes (listed in supplemental Tables 1 and 3) were analyzed by custom-made cDNA macroarrays using cDNA clones from the ABRC and RIKEN BioResource Center (RIKEN BRC; Ibaraki, Japan). Twenty-three genes were redundant between gene sets one and two. These cDNA clones were re-sequenced for confirmation before use. Seventy nanograms of each PCR-amplified sample were blotted onto Hybond N^{+} nylon membranes with Multi Pin Blotter 96 (Atto Co., Tokyo, Japan). Each gene was spotted on a membrane in duplicate. λDNA was used as negative control. The constitutively expressed genes *EF1α* (At5G12110) was included as internal standard. For the macroarray studies, young leaves from both species were harvested after ten weeks of growth in the arid western plant growth protocol with or without 20 μM sodium selenate. Then shoots were separated from roots and frozen with liquid nitrogen for total RNA extraction. Total RNA was extracted from shoots and roots using the RNeasy Plant Mini kit (Qiagen, Valencia, CA, USA). Hybridization, probe labeling and signal detection were carried out according to Tamaoki *et al.* (2003). The signal intensity of each spot was obtained as described previously (Tamaoki *et al.* 2003). In brief, we subtracted the value of the signal intensity of the negative control (λDNA) from the signal intensity of each spot and then normalized the signal intensities against the intensity of *EF1α*, the expression of which had been confirmed to be unchanged with or without 20 μM selenate (see supplemental Figure 4). Macroarray analysis was carried out two times using biological replicate samples, and each macroarray membrane contained duplicate spots for each gene. Thus, the average, standard deviation, and *p*-value of each gene were calculated from fold induction values calculated from four independent spots. From the four independent signal intensities of each spot, we calculated the difference in gene expression between the two *Stanleya* species without selenate (designated as constitutive difference) or with selenate (designated as induced difference). The average, standard deviation, and *p*-value of each gene were calculated from fold induction values using GeneSpring GX10 software (Agilent Technologies, Santa Clara, CA, USA).

Expression analysis via semi-quantitative RT-PCR

Total RNA was isolated from shoots as described above. Five microgram of DNase-treated total RNA was reverse-transcribed using the First Strand cDNA synthesis kit (Fermentas International Inc.; Ontario, Canada), following the manufacturer's instructions. PCR reactions were carried out as described previously (Schiavon *et al.*, 2007). After the separation of each band with agarose gel electrophoresis, the signal intensity of each band was measured with the ImageJ program (NIH). Obtained signal intensities were normalized against the intensity of *EF1α*, a constitutively expressed control gene for RT-PCR. A list of primers used in these experiments is presented as Supplementary Table S5.

Expression analysis via Northern blot analysis

For Northern blot analysis, total RNA was isolated from shoots as described above. An aliquot (10 μg) of each RNA preparation was separated by denaturing agarose gel electrophoresis, transferred onto Hybond N plus membrane (GE healthcare). The cDNA fragments used for hybridization as probes were obtained from the RT-PCR analysis as described above. These cDNA fragments were sequenced for confirmation before use. Probes were made by cutting plasmids with suitable restriction enzymes and then labeled with [α-^{32}P] dCTP. After the hybridization, the signal intensity of each band was measured with the ImageJ program (NIH).

LCMS metabolite quantification

LCMS analysis of organic selenocompounds in plant tissues was performed as described by Freeman et al. (2006). This method does not detect Se that is incorporated in proteins.

LCMS of methyl-jasmonate, salicylate and jasmonate levels in shoot tissue were determined in 10-week old plants grown as described above with or without 20 μM sodium selenate. The extracts were prepared as described by Wilbert et al. (1998). The extracts were analyzed by LC-MS using a Hewlett-Packard Agilent 1100 series HPLC and a Finnigan LcQDuo thermoquest MS system equipped with Xcalibur software. Through 30μL injections these extracts were separated at 40°C using a Phenomenex Hypersil 5-mm C18 (ODS) column (250 X 2 mm, 5 mm) at a flow rate of 0.32 mL/min, using two eluents: (A) water + 0.1% formic acid; and (B) 100% methanol + 0.1% formic acid. The following gradient program was used during the 23 min run: 0-7 min, 50% A and 50% B; 7 - 9 min, 30% A and 70% B; 9 - 12 min, 100% B; 12 -13 min, 50% A and 50% B, with a 10 min post run, column wash 50% A and 50% B.

Standard curves were established using chemicals purchased from Sigma Chemical, St. Louis, MO; Methyl Jasmonate catalog number 392707 had a retention time of 2.5 min, Salicylic Acid catalog number A-6262 had a retention time of 4.45 min, and Jasmonate catalog number J2500 had a retention time of 6.85 min. Through MS, the different metabolites were measured at their appropriate masses and retention times observed for each of the standards. The MS detector settings were 1-3.5 min in positive ion mode using parameters generated with the MeJA standard and the automated tune program, 3.5-5.5 min in negative ion mode using parameters generated with the SA standard and the automated tune program, 5.5-13 min in negative ion mode using parameters generated with the JA standard and the automated tune program. Samples were kept at room temperature (25°C), in the autosampler. The previously published (Wilbert *et al.*, 1998), and observed precursor and product ions for these standards were exactly the same.

GC of ethylene and GCMS of methyl linolenic acid

Gas chromatography (GC) was used to measure ethylene evolution of 5 week old plants, as described by Tamaoki et al. (2008a). Two plants were enclosed into a 60 ml Labco Exetainer® vial (Labco Limited, High Wycombe, UK) for gas chromatographic analysis and incubated for 24 h with illumination in a growth chamber. Ethylene generated during the incubation was measured by injecting 25 mL of headspace gas into a Fisions 8000 gas chromatograph with flame ionization detector (FID). A two meter Altec Hayesep N 80/100 column was used with isothermic oven temperature at 70 °C and flame ionization detection (FID) temperature at 200 °C. The program was 4 min in length with the ethylene peak eluting at 1.40 min. Ethylene peak area was determined by the PeakSimple program (version 3.39, 6 channel; SRI Instruments, Torrance, CA, USA).

Frozen young leaves were extracted for Methyl Linolenate (Me-Lin) analysis by placing 100 mg of frozen tissue into 1 mL of ice-cold ultra pure methanol at 4°C with occasional vortexing until leaves were fully extracted and 100% clear opaque and the methanol was green. Samples were then centrifuged for 10 min at 15,800 x g. Methyl Linolenate was measured using an Agilent 6890 Plus/5973N GC/MS system equipped with a 7683 autosampler tray and autoinjector module with Chemstation software and data system. The column used was a 30 m Supelco SPB-1 column with a 250 μm diameter, a 0.25 μm film thickness, a max temperature of 320°C. Initial flow was 1.0 mL per min with an average velocity of 37 cm/sec and a nominal pressure of 8.64 psi. The elution profile of the oven was a controlled temperature ramp of 70°C at 2 min and 200°C at 20 min with a 320°C 5 min post-run column cleanup. Sample volume injected was 2.0 μL with no post-injection dwell time. Retention time for Me- Lin in leaves was

14.13 min and was quantified using an appropriate standard curve which was established using a standard purchased from Sigma Chemical, St. Louis, MO (catalogue number L2626). Methyl linolenate in leaves from both species matched the Wiley6N mass database used on this GCMS system with an exact 99% quality. The authentic Me Lin standard had the exact same retention time as the plant Me Lin at 14.13 min and also matched the Wiley6N mass database with 99% quality.

Total phenolics content

Leaves were freeze-dried using a Genesis Freeze Drier (Virtis, Inc., Gardiner, NY). Lyophilized samples were then weighed to determine percent dry matter content and ground in preparation for extraction. The dried samples were ground into a fine powder using a mortar and pestle and sieved with a No. 20 Tyler sieve (WS Tyler Inc., Mentor, OH). For sample extraction, 5 mL of 80% acetone (Fisher Scientific, Fair Lawn, NJ) and 200 mg powder from each replicate were placed in 15 mL centrifuge tubes. The tubes were vortexed until thoroughly mixed, rotated in the dark (4˚C) for 15 minutes, then centrifuged (4˚C; 4,000 rpm) for 15 minutes. One mL of supernatant was transferred to an Eppendorf tube and vacufuged at 45˚ C to dryness (approximately 2-3 hours). Samples were stored at -20˚ C until analytical tests were completed. Total phenolics content was measured using a microplate-based Folin-Ciocalteu assay adapted from Singleton et al. (1999), Spanos and Wrolstad (1990), and Esparaza Rivera et al. (2006). Vacufuged extractions were reconstituted with 1.0 mL of 80% acetone, and 100 µL of this solution was diluted with 900 µL nanopure water. In triplicate, 35 µL of the diluted sample was pipetted into microplate wells. Using a multichannel pipette, 150 µL of 0.2 M Folin-Ciocalteu reagent (Sigma-Aldrich, Inc., St. Louis, MO) was added to all wells. The plate was shaken for 30 seconds and held for 5 minutes at room temperature, followed by addition of 115 µL of 7.5% (w/v) Na_2CO_3 (Fisher Scientific) to all wells and rotational shaking for 30 seconds. The plate was held for an additional 5 minutes at room temperature then incubated at 45˚ C for 30 minutes followed by cooling to room temperature for 1 hour. Plates were then read at 765 nm in a Spectra Max Plus (Molecular Devices, Sunnyvale, CA) spectrophotometer using Softmax Pro software (Molecular Devices). Total phenolic content was calculated by comparing to a gallic acid (Sigma Chemical Co., St. Louis, MO) standard curve and expressed as mg/100 g fresh weight (mg GAE/100 g FW).

***In vitro* treatments**

Both *Stanleya* plant species were grown in turface along with the same fertilizer and 20 μM SeO_4^{2-} used in the long term arid drip system. Hormone and elicitors were sprayed onto the shoots, 20 mL daily at 10 μM or 100 μM MeJA or ACC, along with a water control for the last three weeks before the 6-week old *S. pinnata* and *S. albescens* shoots were harvested and dried for Se analyses. *Stanleya pinnata* was then grown in turface and fertilized as described above and 20 μM selenate and hormone and elicitors were sprayed onto the shoots: 20 mL daily five times per week at 10 μM, 100 μM or 500 μM MeJA, JA, SA or ACC, along with a water control for the last two weeks before the 3-week old *S. pinnata* shoots were harvested and dried for Se analyses. Finally, seeds from both plant species were sterilized using 20% bleach and 70% methanol then rinsed 10 times with sterile ddH_2O and germinated on 0.5 strength MS + B5 vitamins with no sucrose. All plants were germinated and grown in the presence of 20 μM SeO_4^{2-} with no added OAS, or with media containing 20 μM SeO_4^{2-} and 50 or 100 μM OAS. After 30 d shoots from both species were harvested and dried for Se analyses.

Acknowledgements

We are grateful to David E. Salt and Wendy A. Peer for their Se hyperaccumulator growth protocol, ITS sequence comparison and chromosome size measurement. We also thank August Bock for providing the SMT antibodies, Donald Dick for helping us with bio-analytical chemistry, and Chris Cohu for helping us with our photosynthetic measurements.

References

Abdel-Ghany SE, Müller-Moulé P, Niyogi KK, Pilon M, Shikanai T (2005) Two P-type ATPases are required for copper delivery in *Arabidopsis thaliana* chloroplasts. Plant Cell **17**: 1233-1251

Al-Turki S, Shahba M, Forsline P, Stushnoff C (2008) Biodiversity of total phenolics, antioxidant capacity and juice quality in apple cider taxa. Hort Environ Biotechnol **49**: 409-417

Assuncao AGL, Martins PDC, Folter SD, Vooijs R, Schat H, Aarts MGM (2001) Elevated expression of metal transporter genes in three accessions of the metal hyperaccumulator *Thlaspi caerulescens*. Plant Cell Environ **24**: 217–226

Barth C, Moeder W, Klessing DF, Conklin PL (2004). The timing of senescence and response to pathogens is altered in the ascorbate-deficient *Arabidopsis* mutant *vitamin c*-1. Plant Physiol **134**: 1784-1792

Bañuelos G, Vickerman DB, Trumble JT, Shannon MC, Davis CD, Finley JW, Mayland, HF (2002) Biotransfer possibilities of selenium from plants used in phytoremediation. Int J Phytorem **4**: 315–331

Beath OA, Gilbert CS, Eppson HF (1939) The use of indicator plants in locating seleniferous soils in the Western United States. I General. Amer J Bot **26**: 257-269

Bert V, Macnair MR, De Laguerie P, Samumitou-Laprade P, Petit D (2000) Zinc tolerance and accumulation in metallicolous and nonmetallicolous populations of *Arabidopsis halleri* (Brassicaceae). New Phytol **146**: 225–233

Boyd RS (2007) The defense hypothesis of elemental hyperaccumulation: status, challenges and new directions. Plant Soil **293:**153-176

Boyd RS, Martens SN (1992) The raison d'etre for metal hyperaccumulation by plants. In AJM Baker, J Proctor, RD Reeves, eds, The Ecology of Ultamafic (Serpentine) Soils. Intercept, Andover, MD, pp 279–289

Broekaert WF, Terras FRG, Cammue BPA, Osborn RW (1995) Plant defensins: novel antimicrobial peptides as components of the host defence system. Plant Physiol **108**: 1353–1358

Brooks RR, Lee J, Reeves RD, Jaffre´ T (1977) Detection of nickeliferous rocks by analysis of herbarium specimens of indicator plants. J Geochem Explor **7**: 49–77

Brown TA, Shrift A (1981) Exclusion of selenium from proteins in selenium tolerant *Astragalus* species. Plant Physiol **67**: 1951–1953

Brown TA, Shrift A (1982) Selenium-toxicity and tolerance in higher plants. Biol Rev (Camb) **57**: 59–84

Byers HG (1935) Selenium occurrence in certain soils in the United States, with a discussion of related topics. US Dept Agric Tech Bull **482**: 1–47

Davis AM (1972) Selenium accumulation in *Astragalus* species. Agron J **6**: 751-754

Davis AM (1986) Selenium accumulation in *Astragalus* and *Lupinus* species. Agron J **78**: 727-729

de Souza MP, Pilon-Smits EAH, Lytle CM, Hwang S, Tai JC, Honma TSU, Yeh L, Terry N (1998) Rate-limiting steps in selenium volatilization by *Brassica juncea*. Plant Physiol **117**: 1487-1494

Dunnill PM, Fowden L (1967) The amino acids of the genus *Astragalus*. Phytochemistry. **6**: 1659-1663

Durrant WE, Dong X (2004) Systemic acquired resistance. Annu Rev Phytopathol **42**: 185-209

Ellis DR, Salt DE (2003) Plants, selenium and human health. Curr Opin Plant Biol **6**: 273–279

Ellis DR, Sors TG, Brunk DG, Albrecht C, Orser C, Lahner B, Wood KV, Harris HH, Pickering IJ, Salt DE (2004) Production of Se-methylselenocysteine in transgenic plants expressing selenocysteine methyltransferase. BMC Plant Biol **4**: 1

Esparaza Rivera, J.R., M.B. Stone, C. Stushnoff, E. Pilon-Smits and P.A. Kendall. (2006) Effects of ascorbic acid applied by two hydrocooling methods on physical and chemical properties of green leaf lettuce stored at 5^0C. Journal of Food Science. **71**: S270-S276

Feist LJ, Parker DR (2001) Ecotypic variation in selenium accumulation among populations of *Stanleya pinnata*. New Phytol **149**: 61-69

Foyer CH, Noctor G (2005) Redox homeostasis and antioxidant signaling: A metabolic interface between stress perception and physiological responses. Plant Cell **17**: 1866–1875

Freeman JL, Lindblom SD, Quinn CF, Marcus MA, Fakra S, Pilon-Smits EAH (2007). Selenium accumulation protects plants from herbivory by Orthoptera via toxicity and deterrence. New Phytol **175**: 490-500

Freeman JL, Quinn CF, Marcus MA, Fakra S, Pilon-Smits EAH (2006b) Selenium tolerant diamondback moth disarms hyperaccumulator plant defense. Curr Biol **16**: 2181-2192

Freeman JL, Quinn CF, Lindblom SD, Klamper EM, Pilon-Smits EAH (2009) Selenium protects the hyperaccumulator *Stanleya pinnata* against black tailed prairie dog herbivory in native habitats. Amer J Bot **96**: 1075-1085

Freeman JL, Zhang LH, Marcus MA, Fakra S, Pilon-Smits EAH (2006a) Spatial imaging, speciation and quantification of selenium in the hyperaccumulator plants *Astragalus bisulcatus* and *Stanleya pinnata*. Plant Physiol **142**: 124-134

Galvis Sanchez, A.C., A. Gil-Izquierdo, and M.I. Gil. (2003) Comparative study of six pear cultivars in terms of their phenolic and ascorbic acid contents and antioxidant capacity. J. Sci. Food Agr. **83**: 995-1003.

Galeas ML, Klamper EM, Bennett LE, Freeman JL, Kondratieff BC, Quinn CF, Pilon-Smits EAH (2008) Selenium hyperaccumulation reduced plant arthropod loads in the field. New Phytol **177**: 715-724

Galeas ML, Zhang LH, Freeman JL, Wegner M, Pilon-Smits EAH (2007) Seasonal fluctuations of selenium and sulfur accumulation in selenium hyperaccumulators and related non-accumulators. New Phytol **173**: 517-525

Garifullina GF, Owen JD, Lindblom SD, Tufan H, Pilon M, Pilon-Smits EAH (2003) Expression of mouse selenocysteine lyase in *Brassica juncea* chloroplasts affects selenium tolerance and accumulation. Physiol Plant **118**: 538-544

Genty B, Briantais JM, Baker NR (1989) The relationship between quantum yield of photosynthetic electron transport and quenching of chlorophyll fluorescence. Biochim Biophys Acta **990**: 87–92

Gomez LD, Noctor G, Knight M, Foyer CH (2004) Regulation of calcium signaling and gene expression by glutathione. J Exp Bot **55**: 1851–1859

Gomes-Junior RA, Gratao PL, Gaziola SA, Mazzafera P, Lea PJ, Azevedo RA (2007) Selenium-induced oxidative stress in coffee cell suspension cultures. Func Plant Biol **34**: 449–456

Goodson CC., Parker R. D., Amrhein C and Zhang Y., (2003) Soil selenium uptake and root system development in plant taxa differing in Se accumulating capability. New Phytol. **159:** 391-401

Hanson B, Garifullina GF, Lindbloom SD, Wangeline A, Ackley A, Kramer K, Norton AP, Lawrence CB, Pilon-Smits EAH (2003) Selenium accumulation protects *Brassica juncea* from invertebrate herbivory and fungal infection. New Phytol **159**: 461-469

Hanson B, Lindblom SD, Loeffler ML, Pilon-Smits EAH (2004) Selenium protects plants from phloem-feeding aphids due to both deterrence and toxicity. New Phytol **162**: 655-662

Horn MJ, Jones DB (1941) Isolation from *Astragalus pectinatus* of a crystalline amino acid complex containing selenium and sulfur. J Biol Chem **139**: 649-660

Jabs T, Dietrich RA, Dangl JL (1996) Initiation of runaway cell death in an Arabidopsis mutant by extracellular superoxide. Science **273**: 1853-1856

Jaffré T, Brooks RR, Lee J, Reeves RD (1976) *Sebertia acuminata*: A hyperaccumulator of nickel from New Caledonia. Science **193**: 579–580

Jost R, Altschmied L, Bloem E, Bogs J, Gershenzon J, Hähnel U, Hänsch R, Hartmann T, Kopriva S, Kruse C, Mendel RR, Papenbrock J, Reichelt M, Rennenberg H, Schnug E, Schmidt A, Textor S, Tokuhisa J, Wachter A, Wirtz M, Rausch T, Hell R (2005) Expression profiling of metabolic genes in response to methyl jasmonate reveals regulation of genes of primary and secondary sulfur-related pathways in *Arabidopsis thaliana.* Photosynth Res **86**: 491-508

Küpper H, Zhao FJ, McGrath SP (1999) Cellular compartmentation of zinc in leaves of the hyperaccumulator *Thlaspi caerulescens.* Plant Physiol **119**: 305–311

Küpper H, Lombi E, Zhao FJ, McGrath SP (2000) Cellular compartmentation of cadmium and zinc in relation to other elements in the hyperaccumulator *Arabidopsis halleri*. Planta **212**: 75–84

Küpper H, Lombi E, Zhao FJ,Wieshammer G,McGrath SP (2001) Cellular compartmentation of nickel in the hyperaccumulators *Alyssum lesbiacum*, *Alyssum bertolonii* and *Thlaspi goesingense.* J Exp Bot **52**: 2291–2300

Krämer U, Grime GW, Smith JAC, Hawes CR, Baker AJM (1997) Micro-PIXE as a technique for studying nickel localization in leaves of the hyperaccumulator plant *Alyssum lesbiacum*. Nucl Instrum Meth Phys Res **130**: 346–350

Laemmli UK (1970) Cleavage of structural proteins during the assembly of the head of bacteriophage T4. Nature **227**: 680-685

LeDuc DL, Tarun AS, Montes-Bayon M, Meija J, Malit MF, Wu CP, AbdelSamie M, Chiang CY, Tagmount A, de Souza M, Neuhierl B, Böck A, Caruso J, Terry N (2004) Overexpression of selenocysteine methyltransferase in *Arabidopsis* and Indian mustard increases selenium tolerance and accumulation. Plant Physiol **135:** 377-383

Lu, Y.R.and L.Y. Foo. (2000) Antioxidant and radical scavenging activities of polyphenols from apple pomace. Food Chemistry **68:** 81-85

Macnair M (1993) The genetics of metal tolerance in vascular plants. New Phytol **8**: 143-148

Macnair MR, Bert V, Huitson SB, Saumitou-Laprade P, Petit D (1999) Zinc tolerance and hyperaccumulation are genetically independent characters. Proc R Soc Lond B Biol Sci **266**: 2175–2179

Marcus MA, MacDowell AA, Celestre R, Manceau A, Miller T, Padmore HA, Sublett RE (2004) Beamline 10.3.2 at ALS: a hard X-ray microprobe for environmental and materials sciences. J Synchrotron Radiat **11**: 239-247

Miller NJ, Rice-Evans CA. (1996) Spectrophotometric determination of antioxidant activity. Redox Report **2**: 161–71

Minguzzi C, Vergnano O (1948) Il contenuto di nichel nelle ceneri di *Alyssum bertolonii* Desv Mem Soc Tosc Sci Nat Ser A **55**: 49–77

Mirouze M, Sels J, Richard O, Czernic P, Loubet S, Jacquier A, François IEJA, Cammue BPA, Lebrun M, Berthomieu P, Marquès L (2006**)** A putative novel role for plant defensins: a defensin from the zinc hyper-accumulating plant, *Arabidopsis halleri*, confers zinc tolerance. Plant J **47**: 329-342

Mou Z, Fan W, Dong X (2003) Inducers of plant systemic acquired resistance regulate NPR1 function through redox changes. Cell **113**: 935–944

Neuhierl B, Thanbichler M, Lottspeich F, Bock A (1999) A family of S-methylmethionine-dependent thiol/selenol methyltransferases. Role in selenium tolerance and evolutionary relation. J Biol Chem **274**: 5407–5414

Neuhierl B, Bock A (1996) On the mechanism of selenium tolerance in selenium-accumulating plants. Purification and characterization of a specific selenocysteine methyltransferase from cultured cells of *Astragalus bisulcatus*. Eur J Biochem **239**: 235–238

Nigam SN, McConnell WB (1969) Seleno amino compounds from *Astragalus bisulcatus* isolation and identification of g-glutamyl-Se-methylseleno-cysteine and Se-methylselenocysteine. Biochim Biophys Acta **192**: 185–190

Nikiforova VJ, Bielecka M, Gakière B, Krueger S, Rinder J, Kempa S, Morcuende R, Scheible WR, Hesse H, Hoefgen R (2006) Effect of sulfur availability on the integrity of amino acid biosynthesis in plants. Amino Acid **30**: 173-183

Parker DR, Laura JF, Varvel TW, Thomason DN, Zhang Y (2003) Selenium phytoremediation potential of *Stanleya pinnata.* Plant Soil **249**: 157-165

Pastori GM, Kiddle G, Antoniw J, Bernard S, Veljovic-Jovanovic S, Verrier PJ, Noctor G, Foyer CH (2003) Leaf vitamin C contents modulate plant defense transcripts and regulate genes that control development through hormone signaling. Plant Cell **15**: 939-951

Peer WA, Baxter IR, Richards EL, Freeman JL, Murphy AS (2005) Phytoremediation and Hyperaccumulator Plants. in: Klomp LWJ, Martinoia E and

Tamás MJ (Eds). Molecular Biology of Metal Homeostasis and Detoxification: from Microbes to Man. Topics in Current Genetics 14, Ch 11. New York, Springer-Verlag.

Penninckx IAMA, Eggermont K, Terras FRG, Thomma BPHJ, De Samblanx GW, Buchala A, Métraux J-P, Manners JM, Broekaert WF (1996) Pathogen-induced systemic activation of a plant defensin gene in Arabidopsis follows a salicylic acid-independent pathway. Plant Cell **8**: 2309–2323

Peterson PJ, Butler GW (1967) Significance of selenocystathionine in an Australian selenium-accumulating plant, *Neptunia amplexicaulis*. Nature **213**: 599 - 600

Peterson PJ, Butler GW (1971) The occurrence of selenocystathionine in *Morinda reticulata* Benth., A toxic seleniferous plant. Austr J Biol Sci **24** : 175-177

Pickering IJ, George GN, Van Fleet-Stalder V, Chasteen TG, Prince RC (1999) X-Ray absorption spectroscopy of selenium-containing amino acids. J Biol Inorg Chem **4**: 791-794

Pickering IJ, Hirsch G, Prince RC, Yu EY, Salt DE and George GN (2003a) Imaging of selenium in plants using tapered metal monocapillary optics, *Journal of Synchrotron Radiation*, **10**: 289-290

Pickering IJ, Prince RC, Salt DE, George GN (2000) Quantitative, chemically specific imaging of selenium transformation in plants. Proc Natl Acad Sci USA **97**: 10717-10722

Pickering IJ, Wright C, Bubner B, Ellis D, Persans M, Yu E,George GN, Prince RC, Salt DE (2003b) Chemical form and Distribution of Selenium and Sulfur in the Selenium Hyperaccumulator *Astragalus bisulcatus*. Plant Phys **131:**1460-1467

Pilon-Smits EAH, Freeman JL (2006) Environmental cleanup using plants: biotechnological advances and ecological considerations. Front Ecol Environ **4**: 230-210

Pilon-Smits EAH, Hwang, S, Lytle CM, Zhu YL, Tai JC, Bravo RC, Chen Y, Leustek T, Norman T (1999) Overexpression of ATP sulfurylase in indian mustard leads to increased selenate uptake, reduction and tolerance. Plant Physiol **119**: 123-132

Quinn CF, Freeman JL, Galeas ML, Klamper EM, Pilon-Smits EAH (2008) The role of selenium in protecting plants against prairie dog herbivory: implications for the evolution of selenium hyperaccumulation. Oeologia **155**: 267-275

Quinn CF, Galeas M L, Freeman JL, Pilon-Smits EAH (2007) Selenium: deterrence, toxicity and adaptation. Integr Environ Assess Manag **3**: 460-462

Rollins R, Rudenberg L (1971) Chromosome numbers of Cruciferae III. Contrib Gray Herb **201**: 117-133

Rollins RC (1939) The cruciferous genus *Stanleya*. Lloydia **2**: 109-127

Reeves, R.D., and Baker, A.J.M. (2000) Phytoremediation of toxic metals. In: Using plants to clean up the environment, Raskin I, Ensley BD, eds (New York: John Wiley & Sons), pp. 193–229

Reeves R, Brooks R (1983) European species of *Thlaspi* L (Cruciferae) as indicators of nickel and zinc. J Geochem Explor **18**: 275-283

Saitoh Y, Imuran N (1987) Active oxygen generation by the reaction of selenite with reduced glutathione in vitro; Joint Japan-USA Congress of Pharmaceutical Sciences Honolulu Hawaii USA December 2-7, J Pharma Sci **76**: S135

Shibagaki N, Rose A, McDermott JP, Fujiwara T, Hayashi H, Yoneyama T, Davies JP (2002) Selenate-resistant mutants of *Arabidopsis thaliana* identify Sultr1;2, a sulfate transporter required for efficient transport of sulfate into roots. Plant J **29**: 475–486

Shrift A, Virupaksha TK (1964) Seleno-amino acids in selenium-accumulating plants. Biochim Biophys Acta **100**: 65–75

Singleton, V.L., Orthofer, R., Lamuela-Raventós, R.M., (1999) Analysis of total phenols and other oxidation substrates and antioxidants by means of Folin-Ciocalteu reagent. In Packer L (ed) Methods in enzymology, Oxidants and antioxidants. Academic Press pp: 152-178

Smirnoff N, Conklin PL, Loewus FA (2001) Biosynthesis of ascorbic acid in plants: a renaissance. Annu Rev Plant Physiol Plant Mol Biol **52**: 437–467

Sors TG, Ellis DR, Salt DE (2005) Selenium uptake, translocation, assimilation and metabolic fate in plants. Photosynth Res **86**: 373-389

Sors TG, Ellis DR, Na GN, Lahner B, Lee S, Leustek T, Pickering IJ, Salt DE (2005) Analysis of sulfur and selenium assimilation in *Astragalus* plants with varying capacities to accumulate selenium. Plant J **42**: 785–797

Sors TG, Martin CP, Salt DE (2009) Characterization of selenocysteine methyltransferases from *Astragalus* species with contrasting selenium accumulation capacity. Plant J **59**: 110-122

Spanos GA, Wrolstad RE (1990) Influence of processing and storage on the phenolic composition of Thompson seedless grape juice. J Agric Food Chem **38**: 1565-1571

Stadtman TC (1996) Selenocysteine. Annu Rev Biochem **65**: 83-100

Stillwell RJ, Berry MJ (2005) Expanding the repertoire of the eukaryotic selenoproteome. Proc Natl Acad Sci USA **102**: 16123–16124

Stushnoff C, Holm D, Thompson MD, Jiang W, Thompson HJ, Joyce NI, Wilson P (2008) Antioxidant properties of cultivars and selections from the Colorado Potato Breeding Program. Amer J Pot Res **85**: 267-276

Tadros TM (1957) Evidence of the presence of an edapho-biotic factor in the problem of serpentine tolerance. Ecology **38**: 14–23

Tamaoki M, Freeman JL, Pilon-Smits EAH (2008a) Cooperative ethylene and jasmonic acid signaling regulates selenate resistance in *Arabidopsis*. Plant Physiol **146**: 1219-1230

Tamaoki M, Freeman JL, Marques L, Pilon-Smits EAH (2008b) New insights into the role of ethylene and jasmonic acid in the acquisition of selenium resistance in plants. Plant Signal Behav **3**: 865-867

Tamaoki M, Matsuyama T, Kanna M, Nakajima N, Kubo A, Aono M, Saji H (2003) Differential ozone sensitivity among *Arabidopsis* accessions and its relevance to ethylene synthesis. Planta **216**: 552-560

Terry N, Zayed AM, de Souza MP, Tarun AS (2000) Selenium in higher plants. Annu Rev Plant Biol **51**: 401-432

Thompson MD, Stushnoff C, McGinley JN, Thompson HJ (2009) *In vitro* measures used to predict anticancer activity of apple cultivars and their comparison to outcomes from a rat model of experimentally induced breast cancer. Nutr Cancer **61**: 510-517

Thompson MD, Thompson HJ, McGinley JN, Neil ES, Rush DK, Holm DG, Stushnoff C (2009) Functional characteristics of potato cultivars (*Solanum tuberosum* L.): Phytochemical composition and inhibition of 1-methyl-1-nitrosourea induced breast cancer in rat. J Food Comp Anal **2**: 571-576

Torres MA, Dangl JL, Jones JDG (2002) Arabidopsis gp91^{phox} homologues AtrbohD and AtrbohF are required for accumulation of reactive oxygen intermediates in the plant defense response. Proc Natl Acad Sci USA. **99**: 517-522

Trelease SF, Beath OA (1949) Selenium. Published by the authors, New York

Trelease SF, Trelease HM (1938) Selenium as a stimulating and possibly essential element for indicator plants. Am J Bot 25: 372–380

Turner JG, Ellis C, Devoto A (2002) The jasmonate signal pathway. Plant Cell **14**: **S153-164**

Van Hoewyk D, Garifullina GF, Ackley AR, Abdel-Ghany SE, Marcus MA, Fakra S, Ishiyama K, Inoue E, Pilon M, Takahashi H, Pilon-Smits EAH (2005) Overexpression of AtCpNifS enhances selenium tolerance and accumulation in Arabidopsis. Plant Physiol **139**: 1518-1528

Vickerman DB, Trumble JT (1999) Feeding preferences of *Spodoptera exigua* in response to form and concentration of selenium. Arch Insect Biochem **42**: 64-73

Virupaksha TK, Shrift A (1965) Biochemical differences between Selenium accumulator and non-accumulator astragalus species. Biochim Biophys Acta **107**: 69-80

Van Hoewyk, D, Takahashi H, Inoue E, Hess A, Tamaoki M, Pilon-Smits EAH (2008) Transcriptome analyses give insights into selenium-stress responses and selenium tolerance mechanisms in Arabidopsis. Physiol Plant **132**: 236-253

Wang KL-C, Li H, Ecker JR (2002) Ethylene biosynthesis and signaling networks. Plant Cell **14**: S131-151

White PJ, Bowen HC, Parmaguru P, Fritz M, Spracklen WP, Spiby RE, Meachan MC, Mead A, Harriman M, Trueman LJ (2004) Interactions between selenium and sulphur nutrition in *Arabidopsis thaliana*. J Exp Bot **55**: 1927–1937

White PJ, Bowen HC, Marshall B, Broadley MR (2007) Extraordinarily high leaf selenium to sulfur ratios define 'Se-accumulator' plants. Ann Bot **100**: 111–118

Wilbert SM, Ericsson LH, Gordon MP (1998) Quantification of jasmonic acid, methyl jasmonate, and salicylic acid in plants by capillary liquid chromatography electrospray tandem mass spectrometry. Anal Biochem **257**: 186-194

Yoshida S, Tamaoki M, Shikano T, Nakajima N, Ogawa D, Ioki M, Aono M, Kubo A, Kamada H, Inoue Y, Saji H (2006) Cytosolic dehydroascorbate reductase is important for ozone tolerance in *Arabidopsis thaliana*. Plant Cell Physiol. **47:** 304-308

Zhang Y, Gladyshev VN (2010) General trends in trace element utilization revealed by comparative genomic analyses of Co, Cu, Mo, Ni and Se. J Biol Chem **285**: 3393-3405

FIGURE LEGENDS

Figure 1. Picture of leaves showing health of each test group after 16 weeks of growth; (A) *S. pinnata* + Se, (B) *S. pinnata* – Se, (C) *S. albescens* + Se, (D) *S. albescens* – Se. Selenium accumulation in leaves after 16 weeks of growth with and without 20 μM SeO_4^{2-} . (E). *S. pinnata* +Se solid triangles, *S. albescens* +Se open triangles, *S. pinnata* -Se solid circles and *S. albescens* -Se open circles ; n = 6 ± SE.

Figure 2. Light intensity-dependent electron transport rate after 16 weeks of growth. *S. pinnata* +Se (solid circles), *S. albescens* +Se (solid squares), *S. pinnata* –Se (open triangles) and *S. albescens* –Se (open diamonds). The relative electron transport rate was calculated from the product of ΦPSII and light intensity (μmol m^{-2} s^{-1}). Data represent the average of 6 different plants ± SD. Significant differences between each treatment and their appropriate controls (grown without Se), using a student's *t* test ($P < 0.05$) are denoted with an asterisk.

Figure 3. Selenium-induced superoxide and hydrogen peroxide visualized by *in situ* ROS stains in 10- week old leaves. Superoxide accumulation in *S. pinnata* + 20 μM SeO_4^{2-} (A), *S. albescens* + 20 μM SeO_4^{2-} (B), monitored *in situ* through the precipitation of purple formazan from the reaction of nitro blue tetrazolium (NBT) with superoxide. Hydrogen peroxide accumulation in *S. pinnata* + 20 μM SeO_4^{2-} (C), *S. albescens* + 20 μM SeO_4^{2-} (D). Hydrogen peroxide was visualized *in situ* as reddish-brown precipitate 3,3'-Diaminobenzidine (DAB).

Figure 4. Quantification of the antioxidants glutathione and ascorbate and the free radical scavenging capacities in *S. pinnata* and *S. albescens* young leaves grown with and without 20 μM SeO_4^{2-}. Glutathione concentrations (nmol g^{-1} fresh weight) (A), distinguishing reduced GSH (open bars) and oxidized GSSG (hatched bars), in plants grown without (–) Se and with (+) Se. Ascorbate (AsA) concentrations (nmol g^{-1} fresh weight) (B) in plants treated without (–) Se (open bars) and with (+) 20 μM SeO_4^{2-} (gray bars). -2,2' Azino-bis (3-ethylbenzo-thiazoline-6-sulfonic acid (ABTS) radical scavenging capacity (μmol Trolox Equivalent Antioxidant Capacity (TEAC) g^{-1} dry weight) (C). 2,2-Diphenyl-1-picrylhydrazyl ($DPPH^*$) radical scavenging capacity (μmol TEAC g^{-1} dry weight) (D). Data represent the average of 3 different plants ± SD. Significant differences using a student's *t* test at $P < 0.05$ are denoted with unique letters.

Figure 5. Immunoblots on total protein extracts from young leaves taken from *Stanleya* pinnata (1-4) and *Stanleya albescens* (5-8) treated with 20 μM SeO_4^{2-}. Blots were decorated with polyclonal antibody raised against the *Astragalus bisulcatus* selenocysteine methyltransferase (SMT) 36.7 KD protein (Neuhierl et al., 1999).

Figure 6. Localization and speciation of Se in *S. pinnata* and *S. albescens*. Micro probe x-ray absorption spectroscopy (μ-XAS) Map showing spatial distribution of total Se imaged in red and Ca imaged in blue both at normal gain, in young leaves of *S. pinnata* (A) and *S. albescens* (B); Bar = 1mm A, B. Insert shows higher magnification image of *S. pinnata* cells containing high levels of Se, area taken from white box.. White circles (A and B) show locations of x-ray absorption near edge structure (XANES) speciation scans reported in Table 3. Scanning electron microscope and energy dispersive spectrometry analysis of the distribution of Se in different tissues (C) exposed by freeze fracturing fully hydrated frozen leaves *Stanleya pinnata* + positive Se detection and - negative Se detection in the various cells. *Stanleya albescens,* showing one single enlarged peripheral epidermal cell (D) + positive for Se; Bar = 50μm. Se distribution in peripheral epidermal cells of *S. pinnata* (E) + positive Se detection; Bar = 30μm. Epidermal cell of *S. pinnata* (F) at higher magnification and light etching of this sample reveals membranes allowing identification of organelles and areas of high Se concentration + positive Se detection and - negative Se detection; Bar = 10μm. Epidermal cell wall of *S. pinnata* (G) without detectable signal - negative for Se; Bar = 10μm. Upper epidermal surface of *S. pinnata* **(**H), a line scan taken across a rupture reveals a positive peak only over a Se-rich epidermal cell immediately beneath the cuticle; Bar = 35μm.

Figure 7. Quantification of the hormones methyl jasmonate (MeJA), jasmonate (JA), their initial precursor methyl linolenic acid, the potent defense response elicitor free salicylic acid (SA), the hormone ethylene and total phenolics in *S. pinnata* and *S. albescens* young leaves grown without (–) Se (open bars) and with (+) 20 μM SeO_4^{2-} (gray bars). MeJA concentrations (A, nmol g^{-1} fresh weight), JA concentrations (B, nmol g^{-1} fresh weight), methyl linolenic acid concentrations (C, μmol g^{-1} fresh weight), free SA (D, nmol g^{-1} fresh weight), ethylene evolution (E, nmol g^{-1} fresh weight hr^{-1}) and total phenolic concentrations (F, expressed as gallic acid equivalents mg g^{-1} dry weight). Data represent the average of 3 different plants ± SD. Significant differences ($P < 0.05$) using a student's *t* test are denoted with unique letters.

Figure 8. Phytohormone and elicitor precursor spray treatments of shoots and O-acetylserine supplemented media caused differential Se accumulation in shoots of *S. pinnata* and *S. albescens*. Daily foliar spray treatments for three weeks of methyl-jasmonate (MeJA) (A), 1-amino-cyclopropane-1-carboxylate (ACC) (B), with water treated controls in comparison to Se accumulation (μg Se g^{-1} leaf dry weight) in 6-week old *S. pinnata* and *S. albescens* shoots. O-acetylserine supplemented growth media v.s. Se accumulation in *S. pinnata* and *S. albescens* μg Se g^{-1} leaf dry weight in 5 week old shoots (C). All plants were germinated and grown throughout in the presence of 20 μM SeO_4 in pre-washed turface with fertilizer or 0.5 strength MS salts + vitamins. Data represent the average of 3-5 different plants ± SD. Significant differences between each treatment and their appropriate water controls using a student's *t* test ($P < 0.05$) are denoted with an asterisk.

Supplemental Figure 1. Root lengths of *S. pinnata* and *S. albescens* grown on vertically placed agar plates after 30 days of growth from germination. Plants treated without (–) Se (open bars) and with (+) 20 μM SeO_4^{2-} (gray bars). Data represent the average of 4-5 different plants ± SE. P-values using a student's *t* test are reported in paragraph 1 of results section.

Supplemental Figure 2. Total non-protein thiols expressed as GSH equivalents (μmol g^{-1} fresh weight) in young and mature leaves of *S. pinnata* and *S. albescens* grown with or without 20 μM SeO_4^{2-}. The only significant difference between treatments in comparison to the other species using a student's *t* test ($P < 0.05$) is denoted with an asterisk.

Supplemental Figure 3. Graphic depiction of the macroarray expression differences from Tables 1-4 and the relative numbers of genes in different categories in young leaves (shoots) and roots of 10-week old *S. pinnata* when compared with *S. albescens* grown with and without 20μM SeO_4^{2-}.

Supplemental Figure 4. Northern Blot and Semiquantitative RT-PCR confirms the gene expression patterns identified in macroarray analysis using a select set of *A. thaliana* probes for genes that showed differences in the macroarray studies. Three genes associated with pathogen defense (*Pin 2*, *AOS* and *PDF 1.2*) and two genes involved in cysteine biosynthesis (CYS synthase and *SAT52*) were all normalized to control *EF1* α (Supplemental Figure 4A). RT-PCR

used a select set of *A. thaliana* primers for genes involved in sulfur metabolism, GSH biosynthesis and pathogen defense that showed differences in the macroarray studies. *EF1* α is used as a constitutive control for RT-PCR (Supplemental Figure 4B). Messenger RNA was isolated from young leaves of 10-week old *S. pinnata* and *S. albescens* with and without 20 µM SeO_4^{2-}. Results quantified using image J are presented in supplemental table 4.

Supplemental Figure 5. A) Liquid chromatographic separation of four authentic seleno-amino acid standards. Mixture of selenomethionine, selenocystine, methylselenocysteine, and γ-glutamyl-methylselenocysteine Mass spectra for γ-glutamyl-methylselenocysteine (gGluMeSeCys) shown with the correct Se isotopic signature. B) Positive mass spectra for Selenocystathionine (SeCyst) with the correct Se isotopic signature. SeCyst is the only free organic selenium compound detected in *S. albescens,* n=3 different plants, young and old leaves. Also not detected (ND) were selenocysteine and selenocystine, negative data not shown.

Table 1. Semi-quantification of SMT immunoreactive band.

Plant species	Mean SMT pixel number ± stderr
Stanleya pinnata	91 ± 36
Stanleya albescens	13 ± 12

1:4000 *A. bisulcatus* SMT antibody, 30µg total protein loaded for each plant.

Table 2. Relative Se protein incorporation coefficient.

Plant species	(Se µg g^{-1} total protein) ÷ leaf Se µg g^{-1}DW
Stanleya pinnata	0.18 ± 0.02
Stanleya albescens	0.13 ± 0.01

Data represent the average n = 3 samples of two different plants pooled.

Table 3. Composition of Se in leaves by microfocused x-ray absorption near-edge structure

Plant species	SeO_4	SeCys	SeCystine	C-Se-C compounds
S.pinnata young leaf	ND	ND	ND	99.5
S.pinnata medium leaf	ND	ND	ND	99.4
S.pinnata old leaf	1.4	ND	ND	98.4
S. albescens young leaf	4.8	19.4	ND	75.5

Se composition calculated from (XANES). Data are average percent of total. n = 3 spectra. ND is not detected.

Table 4A. Constitutive difference (-Se; S.pin/S.alb) 10 week, Shoot, Gene sets 1 and 2					
Gene name	Annotation	Gene ID	Average	SD	p value
Sulfur assimilation genes					
CS26	Cysteine synthase 26	At3g03630	3.45	0.24	0.03
IMPase	Myo-inositol monophosphatase	At4g39120	3.00	0.33	0.03
CYSC1	Cysteine synthase isomer	At3g61440	2.41	0.21	0.02
CS	Cysteine synthase pyridoxal-5'-phosphate-dependent	At1g55880	2.18	0.05	0.01
Antioxidant and redox control genes					
GSTF6	Glutathione-S transferase F6	At1g02930	3.06	0.14	0.01
GRXC10	Glutaredoxin	At5g11930	2.60	0.57	0.08
CAT3	Catalase, putative	At1g20620	2.60	0.47	0.02
mtDHAR	Dehydroascorbate reductase, mitochondrion	At1g19570	2.00	0.45	0.03
GRX	Glutaredoxin	At5g58530	1.95	0.06	0.03
Defense related genes					
PDF1.2	Plant defensin 1.2	At5g44420	31.16	5.11	0.03
PR4	Pathogenesis related protein 4	At3g04720	4.60	0.15	0.00
Pin2	Proteinase inhibitor 2	At2g02100	4.12	0.31	0.03
PR2	Pathogenesis-related protein 2	At3g57260	3.97	0.49	0.01
PR1	Pathogenesis-related protein 1	At2g14610	3.87	0.19	0.01
PR5	Pathogenesis related protein 5	At1g75040	3.76	0.06	0.01
ACS6	1-aminocyclopropane-1-carboxylate (ACC) synthase 6	At4g11280	3.63	0.52	0.04
VSP1	Vegetative storage protein 1	At5g24780	3.02	0.45	0.04
Molecular chaperone genes					
BiP2	Luminal binding protein 2	At5g42020	4.38	0.78	0.02
BiP1	Luminal binding protein 1	At5g28540	3.29	0.64	0.03

Table 4B. Constitutive difference (-Se; S.pin/S.alb) 10 week, Root, Gene set 1					
Gene name	Annotation	Gene ID	Average	SD	p value
Sulfate transporter genes					
Sultr4;1	Sulfate transporter	At5g13550	2.94	0.44	0.03
Sultr1;2	Sulfate transporter	At1g78000	2.84	0.08	0.02
Sultr3;2	Sulfate transporter	At4g02700	2.75	0.04	0.01
Sulfur assimilation related genes					
APR1	5'-adenylylsulfate reductase 1	At4g04610	7.66	0.31	0.02
APS2	ATP-sulfurylase 2	At1g19920	5.14	0.53	0.04
APR3	5'-adenylylsulfate reductase 3	At4g21990	4.79	0.43	0.04
APR2	5'-adenylylsulfate reductase 2	At1g62180	3.23	0.02	0.00
ATMS2	Methionine synthase cytosolic	At3g03780	3.19	0.42	0.02
APS1	ATP sulfurylase 1	At3g22890	3.12	0.03	0.01
OASA1	O-acetylserine (thiol)-lyase	At3g22460	3.09	0.07	0.00
CYSC1	Cysteine synthase isomer	At3g61440	2.92	0.58	0.04
ATMS1	Methioninee synthase cytosolic	At5g17920	2.87	0.46	0.04
ATCYSD2	Cysteine synthase	At5g28020	2.66	0.06	0.01
AKN1	Adenylylsulfate (APS) kinase 1	At2g14750	2.66	0.47	0.04
GSH2	Glutathione synthetase	At5g27380	2.58	0.06	0.02
SAT52	Serine acetyltransferase 52, cytosolic	At5g56760	2.57	0.11	0.01
CYS-3A	cysteine synthase	At4g14880	2.38	0.50	0.05
GSH1	Gamma-glutamylcysteine synthetase	At4g23100	2.55	0.01	0.01
SAT1	Serine acetyltransferase 1, mitochondrial	At3g13110	2.41	0.59	0.05
CS26	Cysteine synthase 26	At3g03630	2.17	0.11	0.01
CYSD1	Cysteine synthase	At3g04940	2.15	0.05	0.00
SAT106	Serine acetyltransferase 106	At2g17640	2.07	0.17	0.02
Antioxidant and redox control genes					
ATFD3	Ferredoxin	At2g27510	4.53	0.49	0.03
GRXS15	Glutaredoxin	At3g15660	3.07	0.28	0.01
GPX2	GSH peroxidase	At2g31570	3.04	0.14	0.02
GRXC10	Glutaredoxin	At5g11930	2.29	0.44	0.04
VTC4	L-galactose-1-phosphate phosphatase, AsA biosynthesis	At3g02870	2.17	0.04	0.03

Defense related genes					
Pin2	Proteinase inhibitor 2	At2g02100	5.10	0.37	0.01
PR5	Pathogenesis related protein 5	At1g75040	3.65	0.43	0.01
VSP1	Vegetative storage protein 1	At5g24780	3.09	0.02	0.01
ACS6	1-aminocyclopropane-1-carboxylate (ACC) synthase 6	At4g11280	2.57	0.21	0.02
PR1	Pathogenesis-related protein 1	At2g14610	2.21	0.02	0.01
Molecular chaperone genes					
HSP17.6-CII	17.6 kDa class II heat shock protein	At5g12020	3.18	0.24	0.04
HSP17.4C-CI	Heat shock protein 17.4 C-CI	At1g53540	2.09	0.09	0.01
Selenoprotein genes					
MZN1.9	Selenoprotein-related	At5g58640	2.08	0.23	0.05
SFP	Selenoprotein family protein	At1g05720	2.93	0.42	0.01
FeS cluster related genes					
CpSufE2	Fe-S metabolism associated domain-containing protein	At1g67810	2.83	0.21	0.01
NFU4	Nitrogen fixation NifU-like family protein	At3g20970	2.22	0.04	0.01
IscA-like 1	HesB-like domain-containing protein	At2g16710	2.29	0.24	0.03
ABA3	Molybdenum cofactor sulfurase family protein	At5g44720	2.77	0.01	0.01
AtMtNifS	Cysteine desulfurase	At5g65720	2.11	0.15	0.03
ISU1	Iron-sulfur cluster assembly complex protein	At4g22220	2.92	0.12	0.01

Table 4C. Induced difference (+Se; S.pin/S.alb) 10 week, Shoot, Gene sets 1 and 2

Gene name	Annotation	Gene ID	Average	SD	p value
Sulfate transporter genes					
Sultr4;1	Sulfate transporter	At5g13550	2.59	0.08	0.02
Sultr1;2	Sulfate transporter	At1g78000	2.30	0.25	0.02
Sultr3;3	Sulfate transporter	At1g23090	2.10	0.01	0.02
Sultr4;2	Sulfate transporter	At3g12520	2.06	0.34	0.06
Sultr2;1	Sulfate transporter	At5g10180	2.08	0.04	0.01
Sulfur assimilation genes					
CYSC1	Cysteine synthase isomer	At3g61440	3.71	0.01	0.02
SAT52	Serine acetyltransferase 52	At5g56760	3.60	0.15	0.04
OASA1	O-acetylserine (thiol)-lyase	At3g22460	2.97	0.54	0.02
IMPase	Myo-inositol monophosphatase	At4g39120	2.50	0.16	0.02
APR3	5'-adenylylsulfate reductase 3	At4g21990	2.42	0.47	0.06
ATCYSD2	Cysteine synthase	At5g28020	2.40	0.52	0.05
Allinase	cysteine sulfoxide lyase, Allinase family protein	At4g24670	2.20	0.08	0.02
AHL	3'-phosphoadenosine-5'-phosphate (PAP) phosphatase	At5g54390	2.19	0.42	0.06
APR1	5'-adenylylsulfate reductase 1	At4g04610	2.12	0.01	0.01
AKN4	Adenylylsulfate (APS) kinase 4	At5g67520	2.08	0.36	0.06
APR2	5'-adenylylsulfate reductase 2	At1g62180	2.07	0.20	0.02
SIR	Sulfite reductase	At5g04590	2.04	0.42	0.06
Antioxidant and redox control genes					
GSTU1	Glutathione-*S* transferase U1	At2g29490	2.56	0.04	0.01
CAT3	Catalase, putative	At1g20620	2.49	0.37	0.01
VTC1	GDP-D-mannose pyrophosphorylase, AsA biosynthesis.	At2g39770	2.38	0.18	0.01
ATFD	Ferredoxin	At1g10960	2.34	0.27	0.03
GPX1	Glutathione peroxidase, chloroplast	At2g25080	2.27	0.06	0.01
GRXS6	Glutaredoxin	At3g62930	2.14	0.24	0.04
ATP2a	Peroxidase 21	At2g37130	2.09	0.37	0.03
CAT1	Cytosolic catalase	At1g20630	2.02	0.04	0.06
Defense related genes					
PDF1.2	Plant defensin 1.2	At5g44420	19.70	4.84	0.05
Pin2	Proteinase inhibitor 2	At2g02100	4.02	0.86	0.04
PR1	Pathogenesis-related protein 1	At2g14610	3.00	0.78	0.04
ACS6	1-aminocyclopropane-1-carboxylate (ACC) synthase 6	At4g11280	2.75	0.53	0.04
VSP1	Vegetative storage protein 1	At5g24780	2.49	0.17	0.01
CRA1	Encodes a 12S seed storage protein	At5g44120	2.37	0.16	0.03
SAL1	3'(2'),5'-bisphosphate nucleotidase, putative	At5g63980	2.22	0.16	0.01
ERD5	Proline oxidase	At5g38710	2.10	0.18	0.04
CNX1	Calnexin 1	At5g61790	2.02	0.37	0.03

CRT1	Calreticulin 1	At1g56340	1.97	0.25	0.02
NPR1	Non-expresser of PR genes 1	At1g64280	1.93	0.03	0.04
Molecular chaperone genes					
HSP17.6-CII	17.6 kDa class II heat shock protein	At5g12020	2.22	0.45	0.05
HSP17.4C-CI	Heat shock protein 17.4 C-CI	At1g53540	2.20	0.01	0.02
HSP17.4A-CI	Heat shock protein 17.4 A-CI	At1g59860	2.16	0.01	0.01
Selenoprotein genes					
SFP	Selenoprotein family protein	At1g05720	2.07	0.04	0.01
SBP	Putative selenium binding protein	At2g03880	2.23	0.15	0.02
FeS cluster related genes					
AtSufE	Sulfur acceptor interacts/activates cysteine desulfurases	At4g26500	2.63	0.71	0.05
NFU4	Nitrogen fixation NifU-like family protein	At3g20970	2.57	0.36	0.06
TIC55	Translocation inner envelope membrane of plastids	At2g24820	2.37	0.11	0.01
ISU1	Iron-sulfur cluster assembly complex protein	At4g22220	2.27	0.42	0.06
ATXDH1	Xanthine dehydrogenase	At4g34900	2.26	0.40	0.05
CpSufD	Fe-S metabolism associated domain-containing protein	At1g32500	2.24	0.08	0.01
AtMtNifS	Cysteine desulfurase	At5g65720	2.08	0.11	0.03
CNX5	Molybdopterin synthase sulphurylase	At5g55130	2.08	0.38	0.06

Table 4D. Induced difference (+Se; S.pin/S.alb) 10 week, Root, Gene set 1

Gene name	Annotation	Gene ID	Average	SD	p value
Sulfate transporter genes					
Sultr3;2	Sulfate transporter	At4g02700	2.28	0.78	0.09
Sulfur assimilation related genes					
IMPase	Myo-inositol monophosphatase	At4g39120	3.29	1.29	0.06
CYSD1	Cysteine synthase	At3g04940	3.19	0.86	0.03
ATMS3	Methionine synthase chloroplastic	At5g20980	2.56	0.23	0.01
APR2	5'-adenylylsulfate reductase 2	At1g62180	2.52	0.74	0.06
CS26	Cysteine synthase 26	At3g03630	2.42	0.06	0.01
SAT52	Serine acetyltransferase 52, cytosolic	At5g56760	2.25	0.18	0.01
APR3	5'-adenylylsulfate reductase 3	At4g21990	2.23	0.46	0.05
ATMS2	Methionine synthase cytosolic	At3g03780	2.15	0.15	0.01
CBL	Cystathionine beta-lyase	At3g57050	2.06	0.24	0.03
Antioxidant and redox control genes					
GRXC9	Glutaredoxin affected by selenium	At1g28480	4.31	0.51	0.00
GRXS15	Glutaredoxin	At3g15660	4.20	0.47	0.01
ATFD3	Ferredoxin	At2g27510	2.66	0.28	0.01
GR2	Glutathione reductase	At3g54660	2.26	0.28	0.02
CXIP2	Glutaredoxin	At2g38270	2.20	0.40	0.03
GRXC5	Glutaredoxin	At4g28730	2.17	0.27	0.03
GRX	Glutaredoxin	At3g57070	2.03	0.27	0.03
Defense related genes					
ACS6	1-aminocyclopropane-1-carboxylate (ACC) synthase 6	At4g11280	3.18	0.88	0.04
Pin2	Proteinase inhibitor 2	At2g02100	2.42	0.40	0.03
GLUT	UDP-glucoronosyl/UDP-glucosyl transferase protein	At1g05680	2.42	0.44	0.02
RD29B	Response to water deprivation, salt and ABA	At5g52300	2.32	0.52	0.04
STZ	Salt tolerance zinc finger	At1g27730	2.28	0.28	0.02
MTN3	Nodulin MtN3 family protein	At5g13170	2.16	0.57	0.05
DDF1	Encodes a member of the DREB subfamily A-1	At1g12610	2.09	0.51	0.06
Molecular chaperone genes					
HSP17.6A	Heat shock protein 17.6A	At5g12030	2.35	0.66	0.06
ATHSP17.4	Heat shock protein 17.4	At3g46230	2.06	0.41	0.05
FeS cluster related genes					
PSAA	Encodes psaA protein reaction center for photosystem I	AtCg00350	3.13	0.13	0.03
NFU2	Nitrogen fixation NifU-like family protein	At5g49940	2.46	0.23	0.02
TIC55	Translocation inner envelope membrane of plastids	At4g25650	2.44	0.87	0.07
TIC55	Translocation inner envelope membrane of plastids	At2g24820	2.29	0.19	0.01
IscA-like 1	HesB-like domain-containing protein	At2g16710	2.27	0.69	0.07

SIRB	Sirohydrochlorin ferrochelatase	At1g50170	2.18	0.56	0.06
PSAC	Encodes the PsaC subunit of photosystem I	AtCg01060	2.07	0.69	0.09
CpSufB	Fe-S metabolism associated domain-containing protein	At4g04770	2.05	0.06	0.03
RDH2	Thiosulfate:cyanide sulfurtransferase	At1g16460	1.99	0.30	0.02

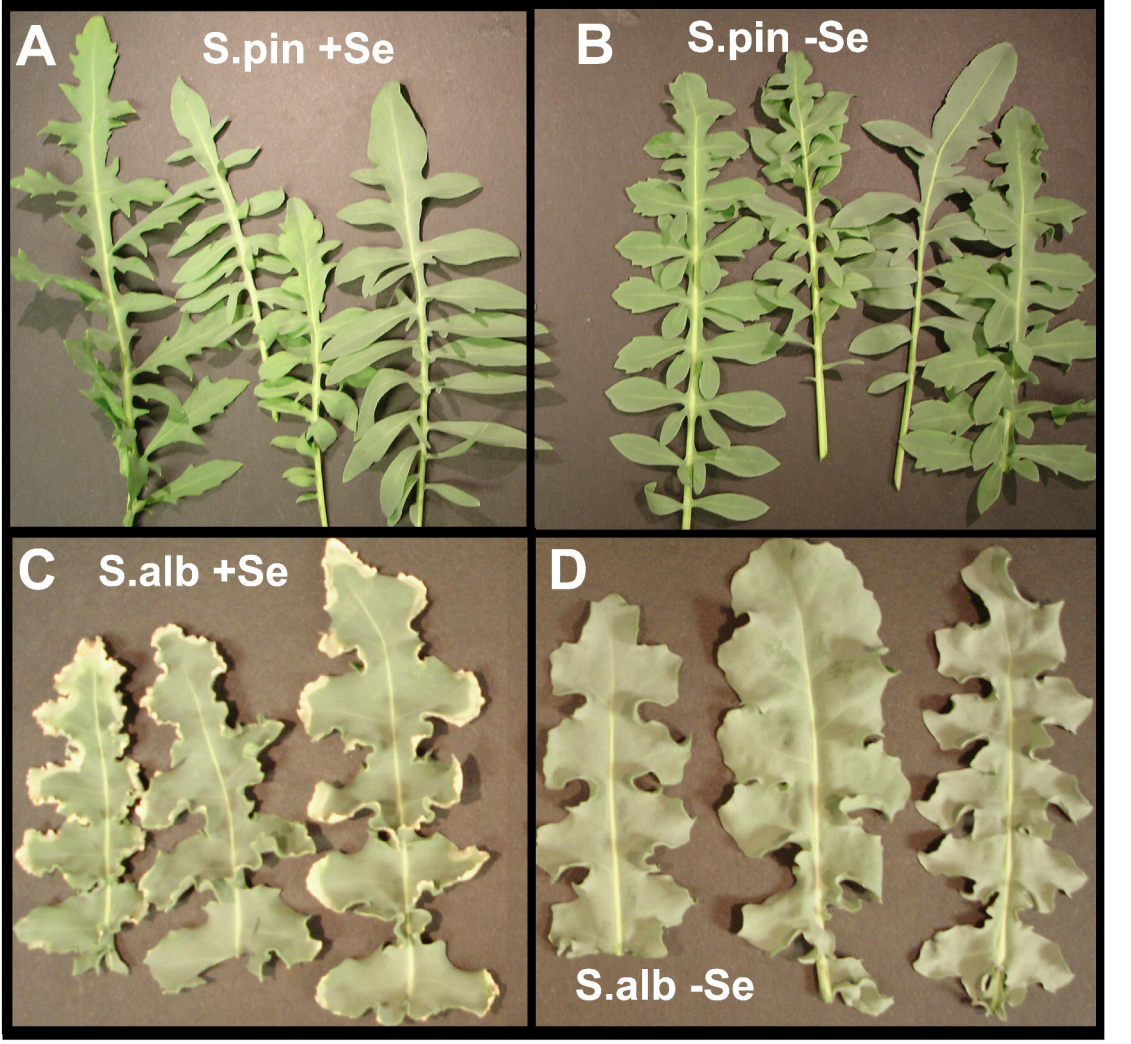
A
S.pin +Se
B
S.pin -Se
C
S.alb +Se
D
S.alb -Se

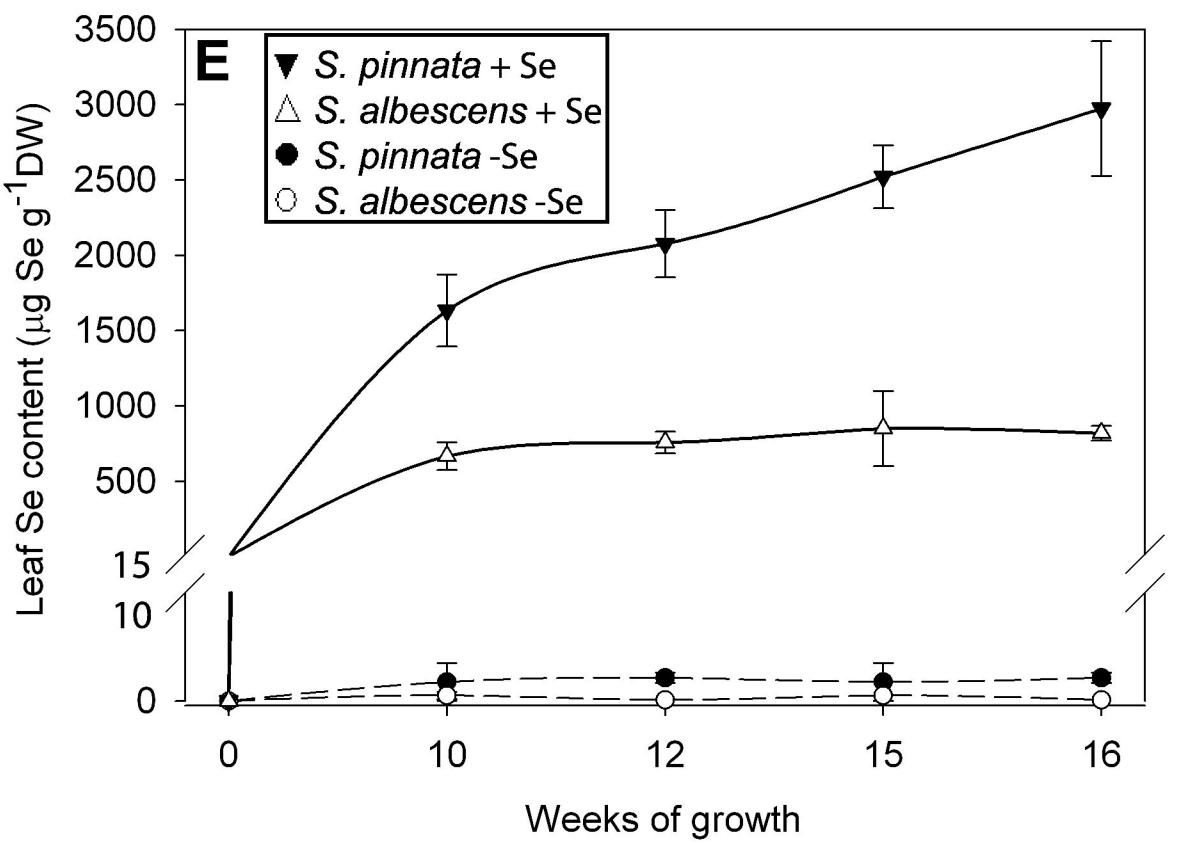
E
S. pinnata + Se
S. albescens + Se
S. pinnata -Se
S. albescens -Se
Leaf Se content (µg Se g-1DW)
3500
3000
2500
2000
1500
1000
500
15
10
0
0
10
12
15
16
Weeks of growth

Figure 1.

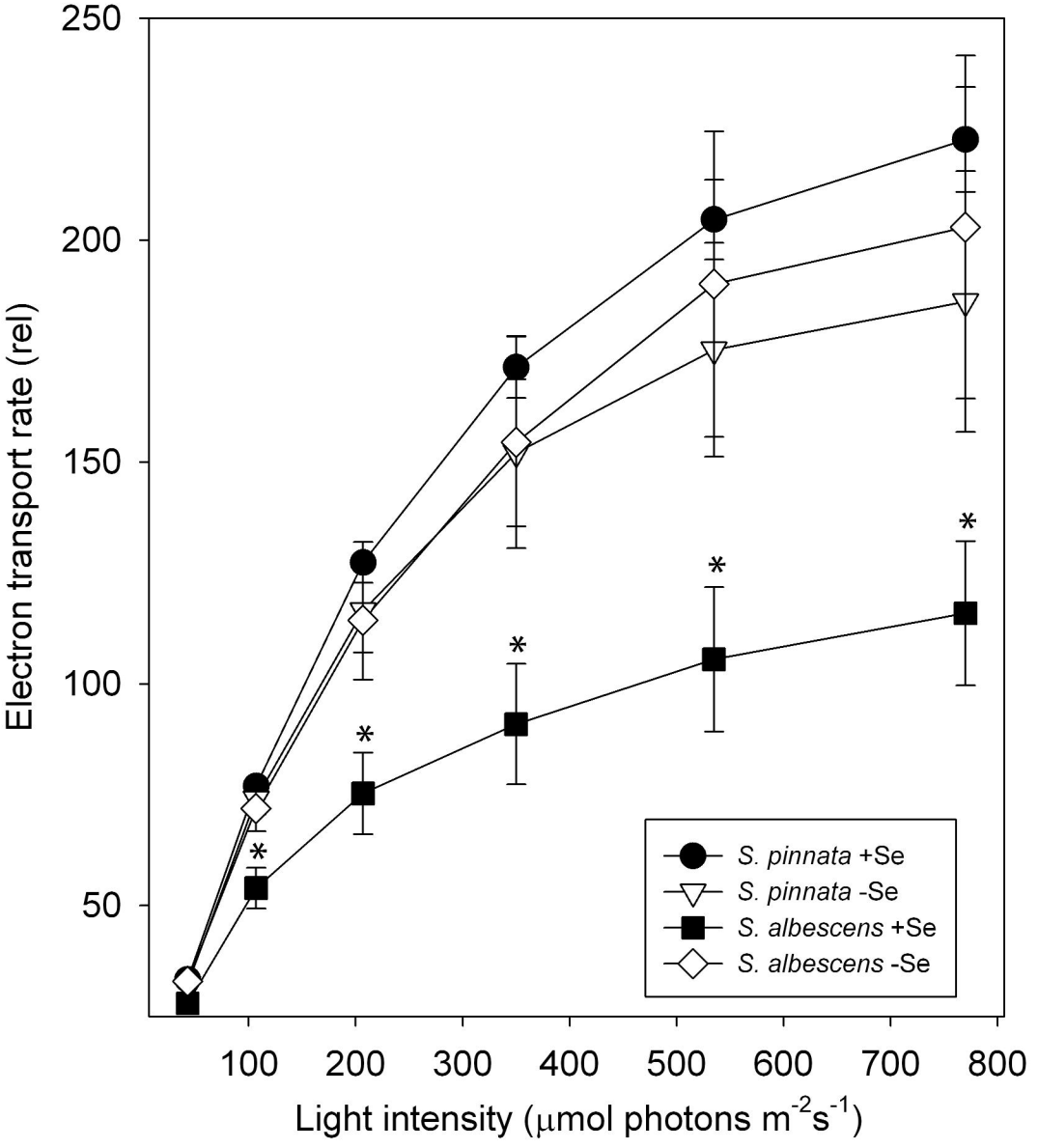
250
200
150
100
50
Electron transport rate (rel)
100
200
300
400
500
600
700
800
Light intensity (μmol photons m-2s-1)
*
*
*
*
*
S. pinnata +Se
S. pinnata -Se
S. albescens +Se
S. albescens -Se

Figure 2.

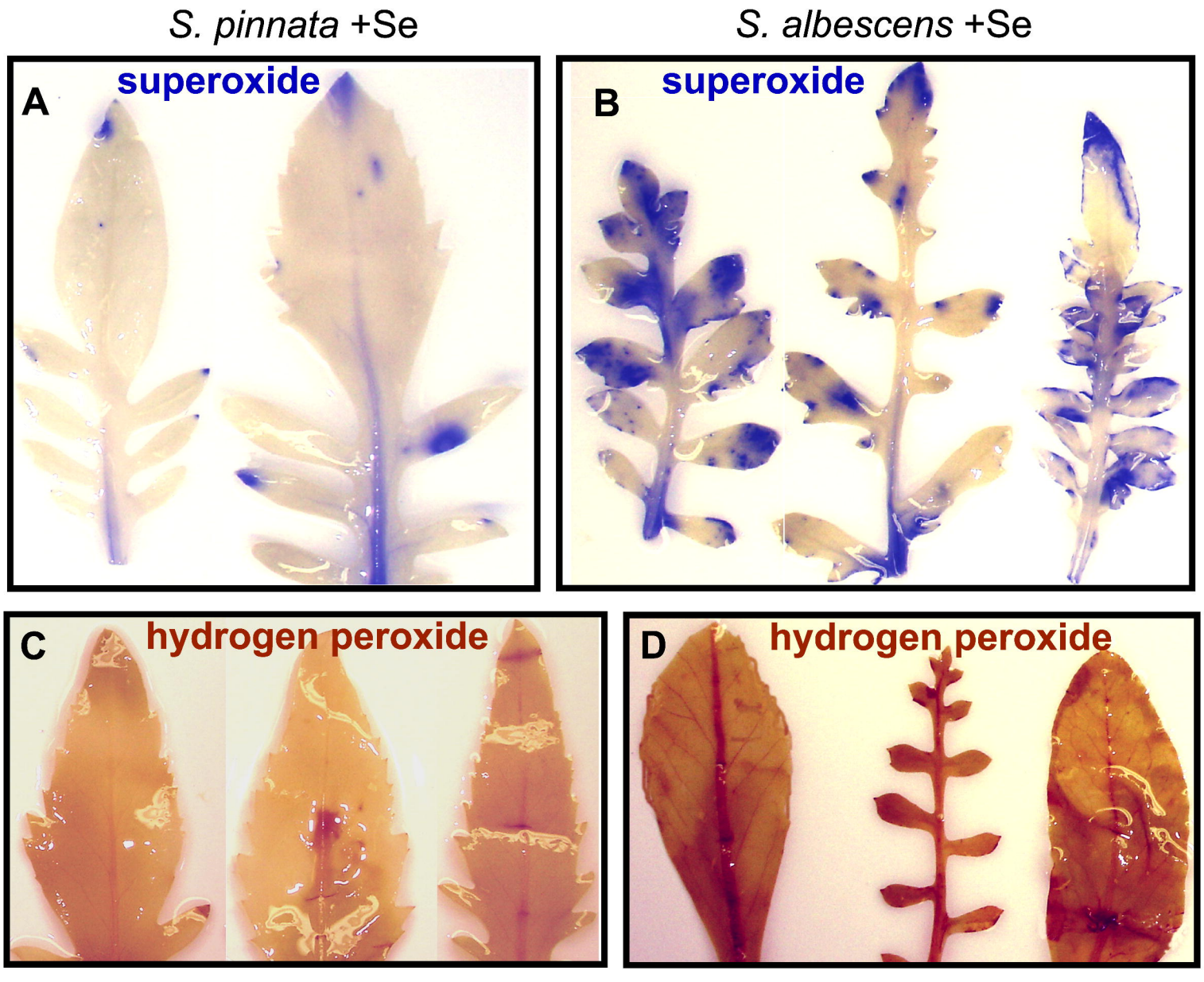
S. pinnata +Se
S. albescens +Se
A
superoxide
B
superoxide
C
hydrogen peroxide
D
hydrogen peroxide

Figure 3.

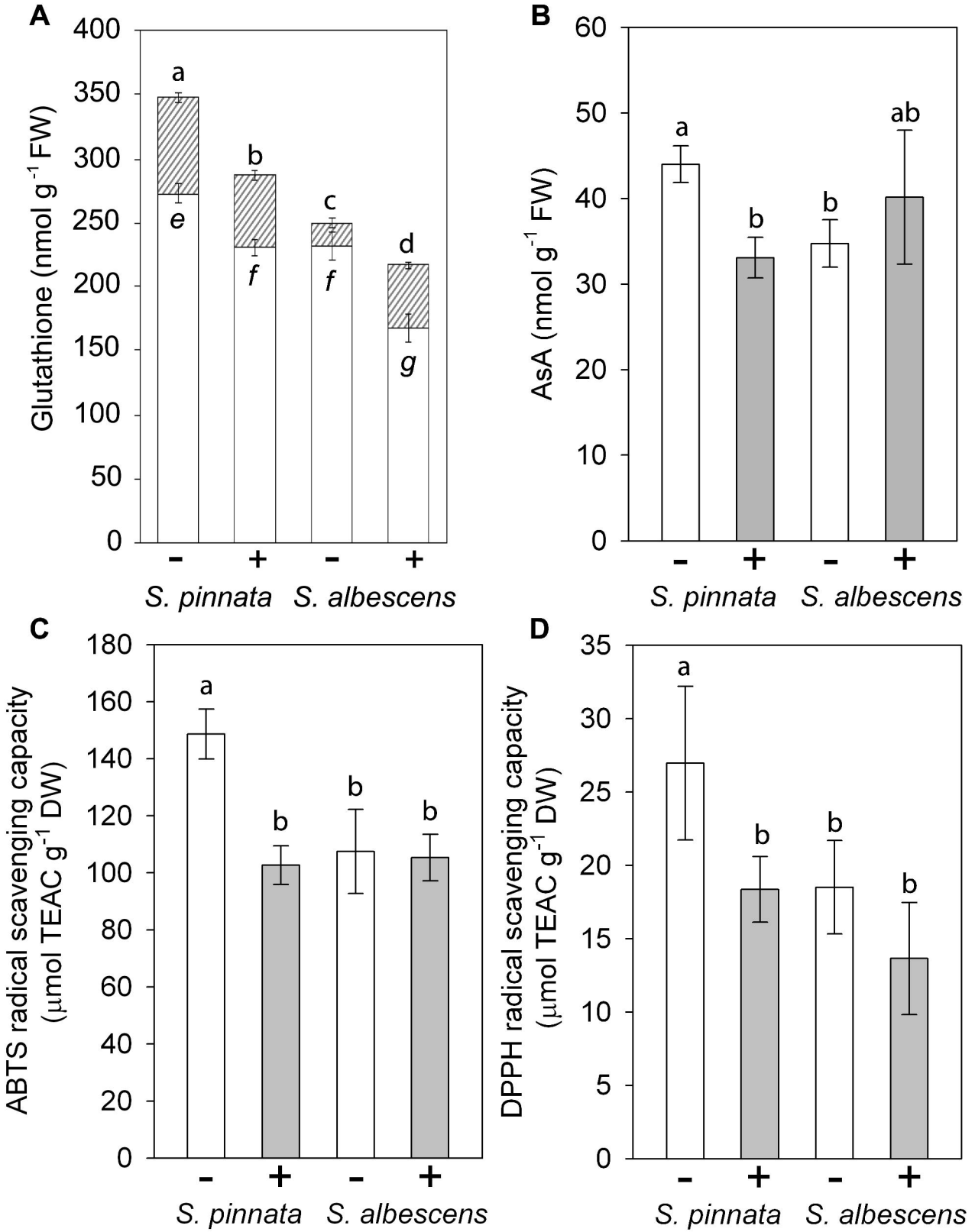
A
Glutathione (nmol g-1 FW)
400
350
300
250
200
150
100
50
0
a
b
c
d
e
f
f
g
-
+
-
+
S. pinnata
S. albescens
B
AsA (nmol g-1 FW)
60
50
40
30
20
10
0
a
b
b
ab
-
+
-
+
S. pinnata
S. albescens
C
ABTS radical scavenging capacity
(µmol TEAC g-1 DW)
180
160
140
120
100
80
60
40
20
0
a
b
b
b
-
+
-
+
S. pinnata
S. albescens
D
DPPH radical scavenging capacity
(µmol TEAC g-1 DW)
35
30
25
20
15
10
5
0
a
b
b
b
-
+
-
+
S. pinnata
S. albescens

Figure 4.

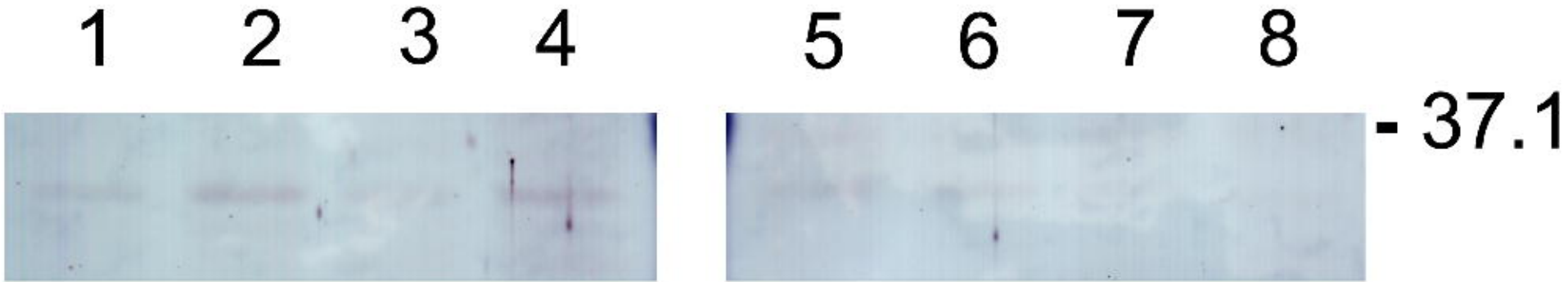

Figure 5.

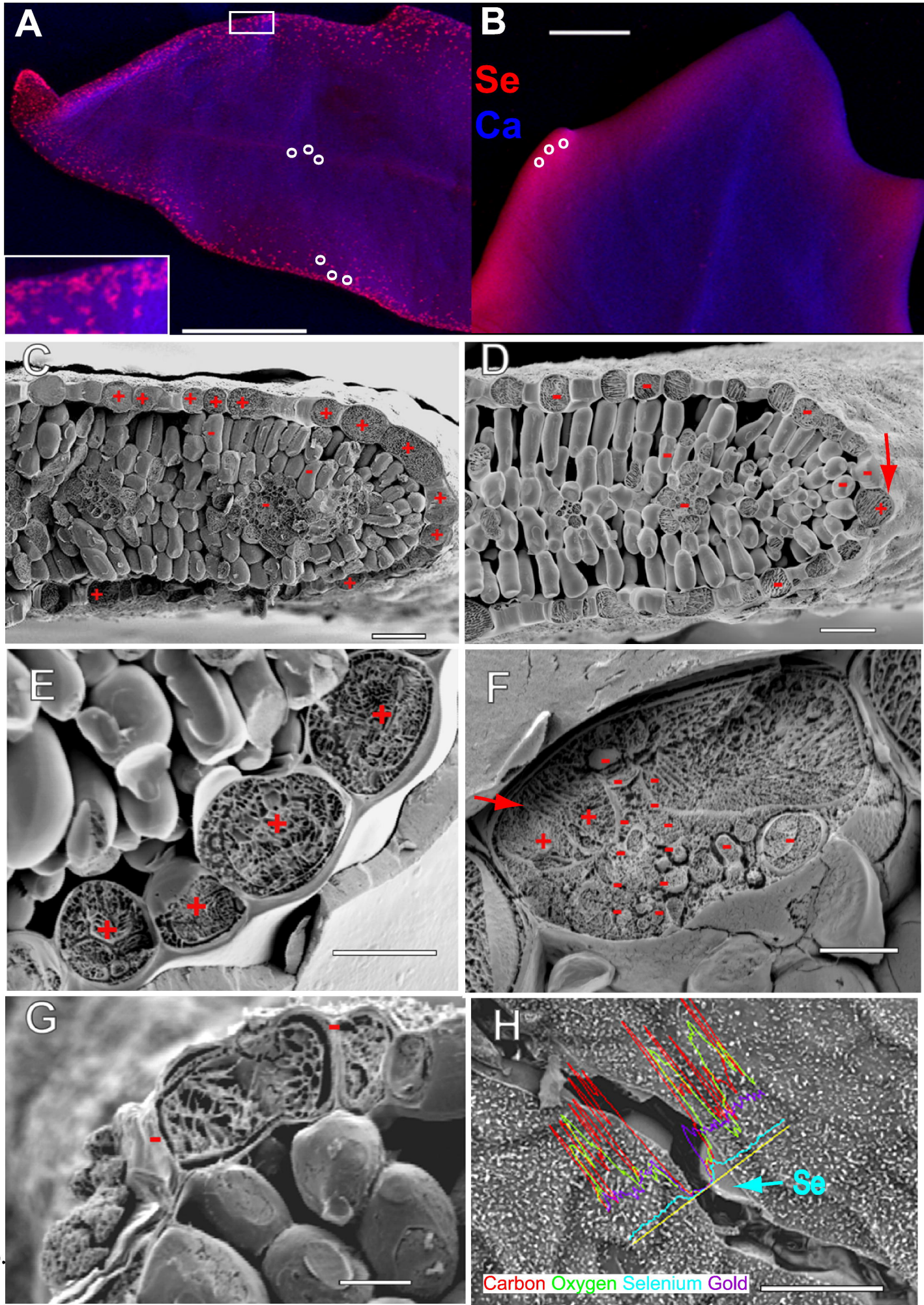

Figure 6.

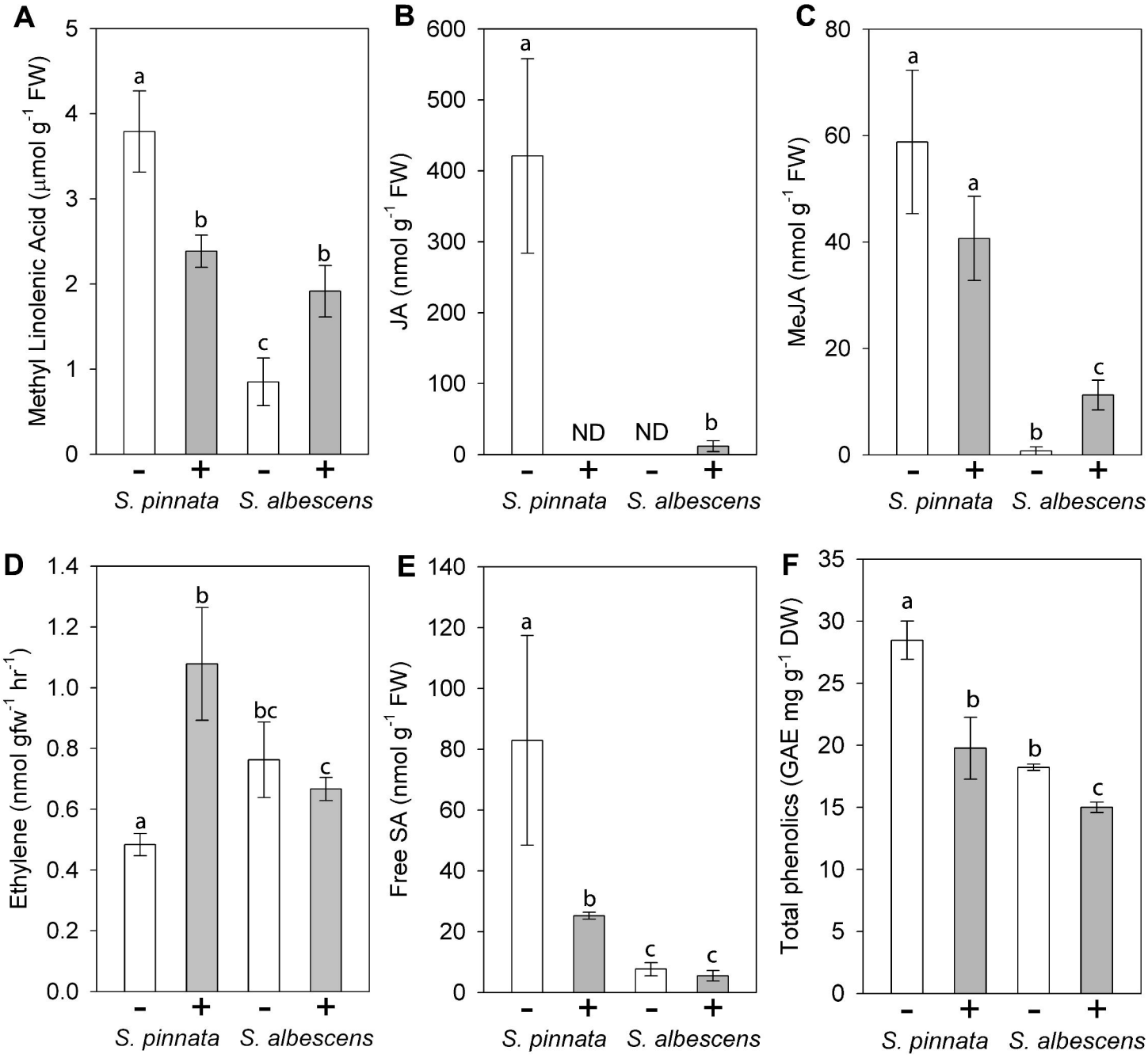
A
Methyl Linolenic Acid (μmol g-1 FW)
0
1
2
3
4
5
a
b
c
b
- + - +
S. pinnata S. albescens
B
JA (nmol g-1 FW)
0
100
200
300
400
500
600
a
ND
ND
b
- + - +
S. pinnata S. albescens
C
MeJA (nmol g-1 FW)
0
20
40
60
80
a
a
b
c
- + - +
S. pinnata S. albescens
D
Ethylene (nmol gfw-1 hr-1)
0.0
0.2
0.4
0.6
0.8
1.0
1.2
1.4
a
b
bc
c
- + - +
S. pinnata S. albescens
E
Free SA (nmol g-1 FW)
0
20
40
60
80
100
120
140
a
b
c
c
- + - +
S. pinnata S. albescens
F
Total phenolics (GAE mg g-1 DW)
0
5
10
15
20
25
30
35
a
b
b
c
- + - +
S. pinnata S. albescens

Figure 7.

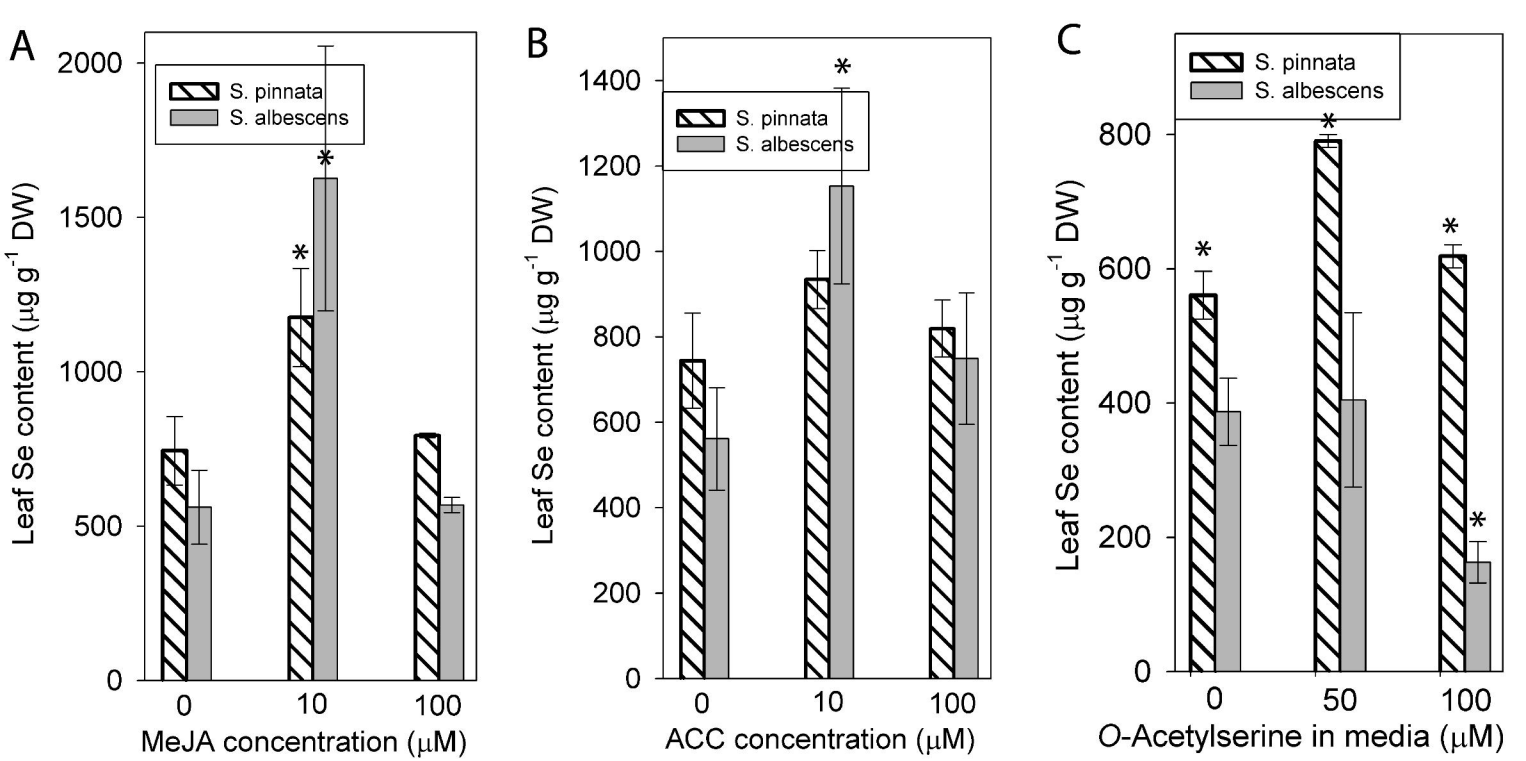
A
B
C
S. pinnata
S. albescens
Leaf Se content (μg g-1 DW)
MeJA concentration (μM)
ACC concentration (μM)
O-Acetylserine in media (μM)
0
500
1000
1500
2000
200
400
600
800
1200
1400
10
100
50
*

Figure 8.